


Article

A Cooperative Lane Change Control Strategy for Connected and Automated Vehicles by Considering Preceding Vehicle Switching

Kang Sun , Xiangmo Zhao, Siyuan Gong * and Xia Wu

School of Information Engineering, Chang'an University, Xi'an 710064, China

* Correspondence: sgong@chd.edu.cn

Abstract: The cooperative lane change among several connected and automated vehicles (CAVs) provides ideas for enhancing the traffic safety and efficiency issues caused by lane changes. However, most of the existing studies mainly focus on the independent analysis of the lateral and longitudinal movements of the lane change without considering the impact of the lateral motion on the longitudinal motion. These works usually assume that the target tracking-preceding vehicles are determined for both the lane change vehicle and the following cooperative vehicle in the target lane. This work proposes a model predictive control (MPC)-based cooperative lane change (CLC) control strategy by considering the preceding vehicle switching and the correlation between the lateral and longitudinal motions. It builds the lateral movement based on the appropriate function curve and integrates this lateral movement in the construction of the coordinated longitudinal motion control strategy by using a set of linear piecewise functions in the design of constraints and objective function of the optimization model to provide smooth preceding vehicles switch. An advanced optimization solver is used to solve the optimization control problem step by step. The proposed strategy is validated based on numerical comparative experiments with two typical lane-changing scenarios. The results show that the proposed control strategy can smoothly complete the preceding vehicle switching during the lane change and quickly realize the stable tracking of the target lane vehicles after changing lanes.



Citation: Sun, K.; Zhao, X.; Gong, S.; Wu, X. A Cooperative Lane Change Control Strategy for Connected and Automated Vehicles by Considering Preceding Vehicle Switching. *Appl. Sci.* **2023**, *13*, 2193. <https://doi.org/10.3390/app13042193>

Academic Editors: Peter Gaspar and Junnian Wang

Received: 6 December 2022

Revised: 30 January 2023

Accepted: 7 February 2023

Published: 8 February 2023



Copyright: © 2023 by the authors. Licensee MDPI, Basel, Switzerland. This article is an open access article distributed under the terms and conditions of the Creative Commons Attribution (CC BY) license (<https://creativecommons.org/licenses/by/4.0/>).

Keywords: cooperative lane change; connected and automated vehicles; model predictive control; preceding vehicle switching

1. Introduction

1.1. Motivations

Lane change activity is one of the most frequent driving behaviors, significantly impacting traffic efficiency [1,2]. Compared with the longitudinal-only car-following behavior, the integration of longitudinal and lateral movement complicates the lane change process. The disturbances caused by lane change eventually lead to traffic congestion, resulting in the elongation of travel time and fuel wastage, thus significantly affecting traffic operation [3]. According to statistics presented in [4], lane-changing maneuvers contribute to approximately 4~10% of the total traffic accidents, which correspondingly leads to a 10% delay in the traffic environment. Furthermore, it is noteworthy that 75% of lane change accidents are directly caused by the wrong decision of the drivers [5].

The ongoing development of the connected and automated vehicle (CAV) technology enabled CAVs to perform collaborative driving with each other on the road [6,7] and showed great potential in addressing the current issues, such as improving safety [8,9], enhancing mobility [10,11], improving traffic efficiency [12,13], and reducing fuel consumption [14,15], via cooperatively controlling CAVs in traffic environment [16]. Most of these approaches leverage the capabilities of CAV and actively collaborate CAVs in different lane

change scenarios to diminish negative effects, such as traffic oscillation or urgent speed change, caused by lane changes [17].

The research works presented in the literature regarding cooperative lane change (CLC) mainly focus on two aspects, i.e., the decision-making strategies before performing a lane change and control strategies in the lane change execution procedure. The decision-making strategies are located on the upper level of a CLC functionality. According to the real-time traffic status of the surrounding environment, these approaches use game theory [18], optimization theory [19,20], and reinforcement learning [21] methods to evaluate the feasibility of lane change gaps in the target lane and the goal of these methods is usually to mitigate the negative impact of the lane change on the traffic flow in the target lane. The control strategies in a CLC functionality will determine the microscopic control law, such as acceleration/deceleration rate and steering wheel angle, for each controlled CAVs in real-time according to the determined lane change gap from the decision-making strategies.

In terms of the controller structure, the control strategies could be classified into two categories, i.e., trajectory planning-tracking and integrated lane change control strategies. The trajectory planning-tracking control strategy is a two-stage controller (i.e., trajectory planning stage and trajectory tracking stage) [22–24]. The trajectory planning stage generates a reference trajectory with the given lane change gap, which satisfies the requirement of safety, comfort, and traffic efficiency [22]. The trajectory tracking stage determines the microscopic control law and makes each CAV follow the reference trajectory given by the planning stage. In addition, better trajectory tracking control should have dynamic adjustment capabilities such as autonomous collision avoidance when the external road environment changes [25,26].

Although the planning-tracking control strategy makes the research problems clear and easy to analyze, it usually includes two layers of optimization models, which not only increases the computational burden of the controller but also leads to weak adaptability to dynamic traffic environment in lane change procedure due to the one-time trajectory generation scheme before lane change executing. Compared with the planning-tracking strategy, the integrated lane change controller combines the trajectory and control law generation in an optimization problem with a set of constraints in safety, physical capability, and comfort [27–30]. Integrated lane change control strategy can be divided into two methods: single-step optimization [28,29] and rolling-horizon optimization control strategies [27,30]. The single-step optimization control strategy is usually given the CLC initial and terminal traffic states. However, the given terminal state of the lane change may make the model less adaptable to the dynamic environment. The rolling-horizon optimization control strategy can solve the optimization iteratively in a given time domain and move forward in time in each solution step, which can improve the adaptability to a dynamic traffic environment.

Even though various CLC control strategies have been studied, some conventional assumptions may impede the further improvement of lane change control strategies in terms of traffic flow efficiency. We discuss three major unrealistic assumptions which motivate this research in the following: (i) most CLC control strategies with independent analysis of lane change mainly focus on the modeling of the longitudinal motions of the controlled CAVs during the lane-changing process and the interaction between the longitudinal and lateral movements of the lane change is not considered [27,30]. However, completely ignoring the influence between the lateral and longitudinal motions may reduce the environmental adaptability of the model. (ii) The preceding vehicle switching process in lane change is oversimplified in those studies. They usually assume no preceding vehicle on the original lane or instantaneously preceding vehicle switch for all controlled CAVs [27–30]. However, the preceding vehicles of the lane-changing vehicle and the following vehicle in the target lane may switch during the lane-changing process. Ignoring the preceding vehicle switching process may lead to a disturbance in the longitudinal controller for the following vehicles in the target lane and may even cause traffic oscillations and traffic accidents in the target lane. (iii) To simplify the problem-solving, most studies usually divide the whole CLC control into two independent stages: lane change control and longitudinal tracking control [27,28,30]. In

fact, after the lane-changing vehicle enters the target lane, it can perform longitudinal tracking adjustment while continuing to execute the lane change lateral motion, so this division is somewhat unreasonable.

Motivated by the aforementioned overlooked assumptions, this paper proposes an MPC-based CLC control strategy for a two-lane highway under a pure CAV traffic flow. In this work, the lane change control is divided into different stages according to the lane in which the lane change vehicle is laterally positioned during the lane change. Based on the architecture of lateral and longitudinal separation of the lane change, the lateral motion of a lane change is described by an appropriate trajectory equation and it is integrated into the process of the longitudinal motion model building. For the longitudinal motion of the lane-changing process, a CLC optimization control strategy is established based on MPC for obtaining the optimal control input of each CAV in real-time. This strategy achieves a safe and effective lane change while considering the correlation between the lateral and longitudinal movements of lane change and preceding vehicle switching of each controlled CAV. In order to verify the performance of the proposed method, two typical lane-changing scenarios are selected to perform a comparative analysis between the proposed model and another separated lane change control strategy. The experimental results show that the proposed method effectively completes the preceding vehicle switching during the lane change and quickly realizes the stable tracking of the target lane vehicles after changing lanes in a pure CAV traffic environment.

1.2. Related Work

As an important part of the CLC maneuver, the CLC control strategies have been studied to control the CAVs for performing safe and smooth lane changes. For the trajectory planning-tracking control strategy, Luo et al. [31] proposed a trajectory planning and tracking scheme for multi-CAVs CLC under multi-lane scenarios. This trajectory planning mode is based on multi-objective optimization problems, and the trajectory tracking mode is based on an MPC controller. Du et al. [32] put forward a cooperative control framework for connected HDVs to cooperate with the CAV to help them carry out safe and efficient lane-changing maneuvers. This research is based on MPC control theory to solve the multi-vehicle interaction and multi-constraint motion-planning problem. For heterogeneous platoons scenarios, Nie et al. [33] proposed a CLC approach for heterogeneous platoons under different communication topologies when the platoon encounters a slow obstacle vehicle ahead. This study first performs trajectory planning for the leading vehicle, and then the platoon vehicles behind the leading vehicle perform simultaneous lane changes using a distributed model predictive control (MPC) algorithm. Wang et al. [34] explored the possibility of accelerating the cooperation of leading vehicles on the target lane and proposed a dynamic CLC control model. Different trajectory planning methods are used in this model for lane change vehicles and cooperative vehicles, but the same trajectory-tracking algorithm was used for all controlled CAVs.

For the integrated single-step optimization control strategy, by considering the concurrent mandatory lane change requirements, Li et al. [29] proposed a CLC trajectory planning method for multiple CAVs by using a nonlinear programming approach with multiple safety and efficiency constraints. For diverging the highway off-ramp, Zheng et al. [35] put forward a cooperative lane-changing strategy to improve traffic operation and safety at a diverging area nearby a highway off-ramp. Based on the cooperative control strategy constructed by the modified Minimizing Overall Braking Induced by the Lane Changes Model (MOBIL) and modified Intelligent Driver Model (IDM) to control the coordination of behaviors between the diverging vehicle and the cooperative vehicle on the target lane. As a typical representative of an integrated rolling-horizon optimization control strategy, MPC has been applied to the field of heterogeneous vehicle platoon control due to its convenient model building and great dynamic control performance [36]. Due to the excellent control effect of MPC in the field of longitudinal platoon control, some scholars have tried to utilize MPC to solve the lateral CLC control problem. To clarify the control process

of lane change, Ni et al. [30] divided the CLC control into two steps, namely feasibility determination and distributed control. An incentive model is used to evaluate the lane change feasibility in terms of acceleration capability and passenger comfort. An MPC-based approach was proposed to collaborate the movement of CAVs. This study [30] divides the complex cooperative lane-changing control process into the lane change phase and the longitudinal headway adjustment phase to predigest the problem-solving of the simplified MPC. Bai et al. [37] presented a CLC motion planning algorithm for partially connected and automated environments. This algorithm reduces the oscillations and shockwaves caused by the lane-changing process.

To summarize, CLC control strategies mainly include trajectory planning-tracking CLC control strategy and integrated CLC control strategy. The integrated CLC control strategies have many advantages over the trajectory planning-tracking CLC control strategies, such as the simplicity of single optimization algorithm structure and dynamic adaptability, so this type of control strategy is used in this study. The current research on integrated CLC control strategy does not consider the longitudinal-lateral correlation of lane change and the switching of controlled vehicles' preceding vehicles, so this study aims to build a more effective CLC control strategy to overcome these shortcomings.

1.3. Contributions

Based on the motivations and literature review, the contributions of this work can be summarized as follows:

- Compared to the current CLC control strategies, which do not consider the lateral and longitudinal correlations of lane change, the proposed CLC control strategy re-associates the mutually independent lane change lateral and longitudinal motions, resulting in a more reliable longitudinal control strategy.
- A series of linear piecewise functions are designed to address the preceding vehicles switching tracking problem. These functions provide a smooth transition for the controlled CAVs (i.e., lane-changing and cooperative vehicles) when their preceding vehicles are changing in the lane-change process.
- Compared with the existing methods of building optimization models sequentially according to different stages of CLC, the proposed CLC control strategy effectively integrates multiple optimization models into a unified model by introducing the preceding vehicle switching method.

Finally, this paper is organized as follows. Section 2 illustrates the problem statement. In Section 3, we present the methodology of the CLC control strategy on a two-lane highway. The numerical simulations are conducted and discussed in Section 4. Finally, this work is concluded in Section 5.

2. Problem Statement

This work proposes a novel CLC control strategy in a pure CAV traffic flow by considering a two-lane highway, as presented in Figure 1. Specifically, we mainly focus on the movements of four vehicles, including the host CAV intending to change lanes (vehicle M) and three surrounding vehicles (vehicles A, B, and C). As presented, vehicles A and B denote the following and preceding vehicles of vehicle M in the target lane, respectively. Vehicle C is the preceding vehicle of vehicle M in the original lane. The longitudinal position, speed, and acceleration of vehicle i (where $i = \{M, A, B, C\}$) are denoted as x_i , v_i , and a_i , respectively. Vehicle M obtains the aforementioned motion state information in real-time based on onboard sensors and V2V communication. Vehicle M leaves the original lane behind vehicle C and enters the target lane when the gap constraint between vehicles A and B is satisfied.

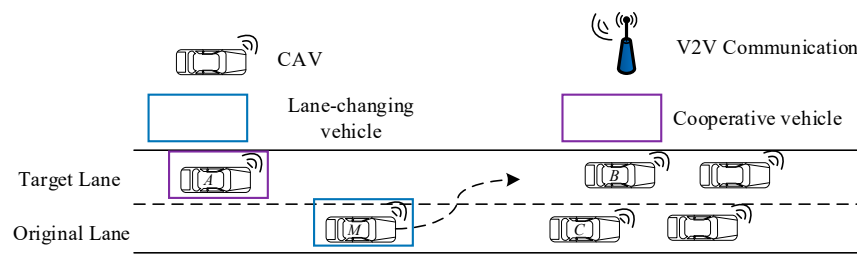


Figure 1. The CLC scenario on a two-lane highway.

Since vehicles B and C are driving with free flow states forming a stable car-following state with their preceding vehicles, there may not be enough space for coordinated control. Therefore, if vehicle M sends a CLC request in its ambient area, vehicle A can act as the cooperative vehicle employing V2V communication to form a cooperative relationship with vehicle M. Based on the aforementioned lane-changing scenario, vehicle A provides suitable space for vehicle M for changing lanes by adjusting its speed to improve the success rate of lane change of vehicle M. Additionally, the vehicle M ensures a safe gap from vehicle C by adjusting its speed. When vehicle M is about to leave the original lane and enter the target lane, vehicles A and M should update their tracked preceding vehicles, i.e., switching from vehicles M and C to vehicles M and B, respectively, and reach their expected motion state without disturbing the traffic flow. Based on the previous description, we divide the whole lane-changing process into two stages, including the lane change process in the original lane (LC-O) stage and the lane change process in the target lane (LC-T) stage, as presented in Figure 2. The LC-T stage follows the LC-O stage and includes its subsequent car-following phase after the lane change vehicle enters the target lane.

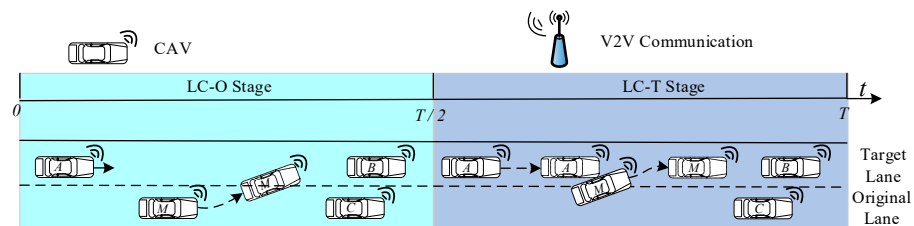


Figure 2. The two stages of the lane change.

During the lane-changing process, vehicle M performs both lateral and longitudinal movements. At the same time, vehicle A adjusts its longitudinal motion based on the CLC control strategy. In this work, the longitudinal accelerations of vehicles M and A are coordinately determined by the proposed optimization model. The proposed model considers the disturbance produced by a lane change maneuver and its negative effect on an ambient area. On the other hand, the lateral acceleration changes according to an appropriate lateral motion trajectory model. During the LC-O stage, vehicle M collaborates with vehicle A to ensure that the vehicle M enters in the target lane safely and effectively on the premise of less impact on the traffic flow of the target lane. In the LC-T stage, vehicle M gradually enters in the target lane and drives in cooperation with vehicle A to achieve the desired car-following states among vehicles M, A, and B.

In order to further support the proposed approach, we make the following assumptions:

- (1) All the CAVs involved in this work can share real-time information accurately and timely based on V2V communication [38]. It is assumed that there is no packet loss and communication delay during the process of information sharing.
- (2) The CAVs are equipped with high-precision onboard sensors, which can accurately measure the position, speed, and acceleration of the vehicles.
- (3) This work adopts a lateral and longitudinal separation structure [30,39].
- (4) Vehicles M and A follow the same upper and lower bounds of acceleration constraints.

- (5) The control command of CLC is obtained by the central control vehicle and sent to each vehicle for execution.
- (6) Vehicle M is at the centerline of the original lane before making a lane change and is also at the target lane's centerline after the lane change's completion.

3. Modeling Methodology

The lane-changing process of vehicle M is composed of two parts. The lateral movement is mainly expressed by the existing mature trajectory function, whereas the longitudinal movement is discussed in detail as the key point of the CLC control strategy, and the construction of the optimization model is studied in this section.

3.1. Lateral Control for the Lane Change Vehicle

In the lateral direction, safety and comfort during driving should be considered when designing the lane change trajectories. Therefore, the selected lane-changing trajectory is required for smoothness, continuity, and easy generation. In this work, the sine function is used to determine the lateral trajectory [40], which has a continuous second derivative and is easy to construct. The lateral acceleration is expressed based on the sine function as follows:

$$a_y(t) = \begin{cases} \frac{2d\pi}{T^2} \sin\left(\frac{2\pi}{T}t\right) & \text{if } 0 \leq t \leq T \\ 0 & \text{otherwise} \end{cases} \quad (1)$$

The duration of the lateral movement during the entire lane-changing process is T . The lateral displacement is obtained by integrating the lateral acceleration $a_y(t)$ twice:

$$y_M(t) = \begin{cases} \frac{d}{T}t - \frac{d}{2\pi} \sin\left(\frac{2\pi}{T}t\right) & \text{if } 0 \leq t \leq T \\ d & \text{otherwise} \end{cases} \quad (2)$$

Since vehicle M performs a lane change from the center line of the original lane to the center line of the target lane, as shown in Figure 3, its lateral displacement exactly equals the lane width d . In accordance with the industry standard of road construction in China, in this work, the lane width d is 3.5 m. Based on the law of the sine function, vehicle M moves to the boundary of two lanes at time $t = T/2$, which is regarded as the moment at which vehicle M leaves the original lane and begins to enter the target lane.

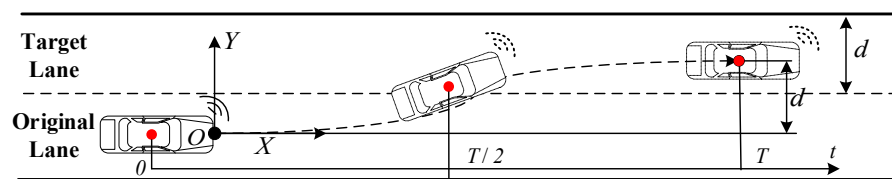


Figure 3. Lateral movement of lane change vehicle.

3.2. MPC-Based CLC Control Strategy by Considering Preceding Vehicle Switching

During the lane-changing process, the host vehicle M and the cooperative vehicle A adjust their longitudinal motions based on the proposed control strategy [41]. In order to ensure the safe and smooth implementation of lane change, a multi-objective collaborative optimization control problem is constructed, which considers the safety, comfort, and traffic efficiency of the upstream traffic in the target lane.

In the proposed optimization model, vehicle M and vehicle A are considered as the optimization objects. The preceding vehicles in the target and original lanes, i.e., vehicles B and C, are considered to be uncontrolled vehicles that impact the safety of vehicles M and A. The optimization objective is to achieve safe and effective lane change and reduce the negative impact on the traffic flow in the target lane by cooperating with the two controlled vehicles A and D with consideration of preceding vehicle switching.

3.2.1. Vehicle Dynamics

This work mainly focuses on the longitudinal motion of the vehicles. Therefore, the classical linear vehicle kinematic model for vehicle longitudinal dynamics is used for the implementation of the proposed strategy. The lane-changing vehicle M and the cooperative vehicle A only possess the longitudinal motions and is expressed by the following equation:

$$\begin{cases} \dot{x}_i = v_i \\ \dot{v}_i = a_i \end{cases} \quad i = M, A \quad (3)$$

As the linearization process may reduce the accuracy of the model, this study discretizes the longitudinal motion model of vehicles M and A. The results of discretization are expressed as follows:

$$\begin{cases} x_i(k+1) = x_i(k) + v_i(k)dt + a_i(k)dt^2/2 \\ v_i(k+1) = v_i(k) + a_i(k)dt \end{cases} \quad i = M, A \quad (4)$$

where dt is the sampling interval.

3.2.2. Constraints with Preceding Vehicle Switching of CLC Control Strategy

(1) Speed limitation

First, the longitudinal speed of vehicle M and its cooperative vehicle A should not exceed the maximum allowable speed in their current lanes, and they should always be positive.

$$0 < v_M(k) \leq \begin{cases} v_{Omax} & \text{if } 0 \leq y_M(k) \leq d/2 \\ v_{Tmax} & \text{otherwise} \end{cases}, \quad k = 1, 2, \dots, N \quad (5)$$

$$0 < v_A(k) \leq v_{Tmax}, \quad k = 1, 2, \dots, N \quad (6)$$

where $v_M(k)$ and $v_A(k)$ represent the longitudinal speeds of vehicles M and A, respectively, and v_{Omax} and v_{Tmax} represent the maximum allowable speeds in the original and target lanes, respectively.

(2) Longitudinal safety distance requirements with preceding vehicle switching

Second, the longitudinal distance between the controlled vehicles, i.e., vehicles M and A, should be more than the corresponding critical longitudinal safety distance during the two stages of the whole lane-changing process. In the LC-O stage, the main movement area of vehicle M is the original lane. So, the tracking-preceding vehicles of controlled vehicles M and A are vehicles C and B, respectively. In order to ensure a safe lane-changing process, the longitudinal safety distance constraints between vehicles C and M and vehicles B and A should be satisfied. These constraints are expressed using (7) and (8), respectively. Please note that the critical longitudinal safety distance is fixed due to the advantages of high-precision and high-response control of CAVs.

$$S_{CM}(k) = x_C(k) - x_M(k) \geq S_{safe, CM}(k) = d_0, \quad k = 1, 2, \dots, N \quad (7)$$

$$S_{BA}(k) = x_B(k) - x_A(k) \geq S_{safe, BA}(k) = d_0, \quad k = 1, 2, \dots, N \quad (8)$$

where $*(k)$ denotes the related predicted state at step k , $S_{CM}(k)$, $S_{BA}(k)$, $S_{safe, CM}(k)$, and $S_{safe, BA}(k)$ represent the actual longitudinal distance and the critical longitudinal safety distance between vehicles C and M, and vehicles B and A, respectively, $x_C(k)$, $x_M(k)$, $x_B(k)$, and $x_A(k)$ represent the longitudinal positions of vehicles C, M, B, and A, respectively, and d_0 represents the fixed minimum safety distance.

In the LC-T stage, the area where vehicle M is located in the target lane, the tracking-preceding vehicles of controlled vehicles M and A are switched from vehicles C and B to vehicles B and M, respectively. Therefore, the safe longitudinal distance constraints between

vehicles B and M, and vehicles M and A should also be guaranteed. These constraints are mathematically expressed in (9) and (10).

$$S_{BM}(k) = x_B(k) - x_M(k) \geq S_{safe, BM}(k) = d_0, k = 1, 2, \dots, N \quad (9)$$

$$S_{MA}(k) = x_M(k) - x_A(k) \geq S_{safe, MA}(k) = d_0, k = 1, 2, \dots, N \quad (10)$$

where $S_{BM}(k)$, $S_{MA}(k)$, $S_{safe, BM}(k)$, and $S_{safe, MA}(k)$ represent the actual longitudinal distance and the critical longitudinal safety distance between vehicles B and M, and vehicles M and A, respectively.

The aforementioned analysis shows that if the expressions presented in (7)–(10) are satisfied, then the driving safety of the four vehicles in two stages of the lane-changing process is ensured. However, it is noteworthy that these constraints are independent of each other and do not consider the switching problem for the preceding vehicles M and A. In addition, these constraints consider that the tracking of vehicles M and A can show sudden changes. Therefore, establishing an optimization problem based on the premise of a sudden change of the preceding vehicles for the controlled vehicles may lead to unsolvable optimization problems.

In reality, vehicle M moving from the original lane to the target lane is a gradual process instead of being an instantaneous process. Let us consider vehicle A as an example; if the instantaneous constraint switching is applied, the longitudinal safety constraint between vehicles M and A is only satisfied during the LC-T stage but not during the LC-O stage. Consequently, vehicle A is unable to provide a safe lane-changing gap for vehicle M to change lanes at the beginning of the LC-T stage. On the other hand, the sudden switching of constraints may also cause drastic speed changes, thus affecting comfort. The longitudinal safety constraint between vehicles M and A should change gradually with the lateral movement of vehicle M. Therefore, a suitable preceding vehicle switching method is needed to cope with the above problems. Studies have been conducted to apply switching control methods to connected and automated vehicle platoon control and showed superior performance in cooperative driving of heterogeneous nonlinear vehicle platoons [42]. Inspired by the above study, to ensure both the traffic efficiency and the applicability of the proposed CLC control strategy, two linear piecewise functions are designed, as presented in (11) and (12). These functions are integrated in the longitudinal safety constraints of LC-O and LC-T, as presented in (13)–(14) and (15)–(16), respectively. As a result, the constraints can be updated smoothly with the lateral motion of vehicle M.

$$LPFA(k) = \begin{cases} L_1 & \text{if } 0 \leq y_M(k) \leq d/2 \\ L_1 - L_2[y_M(k) - d/2] & \text{otherwise} \end{cases}, k = 1, 2, \dots, N \quad (11)$$

$$LPFB(k) = \begin{cases} L_3 y_M(k) & \text{if } 0 \leq y_M(k) \leq d/2 \\ L_4 & \text{otherwise} \end{cases}, k = 1, 2, \dots, N \quad (12)$$

During the LC-O stage, we have:

$$S_{CM}(k) \geq S_{safe, CM}(k) LPFA(k), k = 1, 2, \dots, N \quad (13)$$

$$S_{BA}(k) \geq S_{safe, BA}(k) LPFA(k), k = 1, 2, \dots, N \quad (14)$$

During the LC-T stage, we have:

$$S_{BM}(k) \geq S_{safe, BM}(k) LPFB(k), k = 1, 2, \dots, N \quad (15)$$

$$S_{MA}(k) \geq S_{safe, MA}(k) LPFB(k), k = 1, 2, \dots, N \quad (16)$$

where $y_M(k)$ denotes the actual lateral distance of vehicle M from the centerline of the original lane. $LPFA(k)$ is a function that first maintains a constant value and then decreases with a fast speed to a large negative value with the variation of the lateral position of vehicle M. In $LPFA(*)$, L_1 and L_2 denote the control parameters, L_1 is a positive value equal to

1 and L_2 is a large negative value. $LPFB(*)$ is a function that first increases and then maintains a constant value. Its value rises gradually from 0 to 1 and then remains 1 with the variation of the lateral position of vehicle M. L_3 and L_4 denote the control parameters of $LPFB(*)$, which are positive values and equal to $2/d$ and 1, respectively.

The shape of $LPFA(*)$ is presented in Figure 4. It changes with the lateral position of vehicle M, i.e., $y_M(k)$. In the LC-O stage, i.e., $0 \leq y_M(k) \leq d/2$, the value of the function that $LPFA(*)$ maintains 1. In the LC-T stage, i.e., $y_M(k) > d/2$, the value of $LPFA(*)$ decreases with a fast speed to a large negative value.

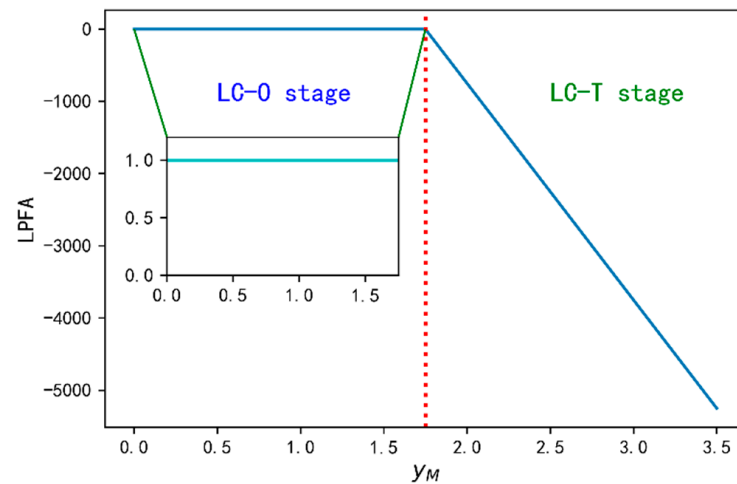


Figure 4. The trajectory curve of linear piecewise function $LPFA$.

In order to explain the physical meaning of introducing a linear piecewise function, i.e., $LPFA(*)$, in the longitudinal safety distance constraint, the longitudinal distance constraint between vehicles C and M, presented in (13) is illustrated as an example. By introducing $LPFA(*)$, the right side of inequality (13), i.e., $S_{safe,CM}(k)LPFA(k)$, maintains $S_{safe,CM}(k)$ in the LC-O stage, thus indicating that the longitudinal distance constraint between vehicles C and M should always be held in this stage. This physically shows that vehicle C always has an impact on the longitudinal motion of vehicle M in this stage. In the LC-T stage, the right side of inequality $S_{safe,CM}(k)LPFA(k)$ decreases rapidly from $S_{safe,CM}(k)$ to a large negative value. Physically, vehicle M has moved into the target lane and vehicle B has become the new preceding vehicle of vehicle M in this stage and influences the longitudinal motion of vehicle M. Similarly, vehicle C no longer influences the longitudinal motion of vehicle M. Therefore, the right side of the inequality (13), i.e., $S_{safe,CM}(k)LPFA(k)$, is quickly replaced by a negative value. Mathematically, the function $LPFA(*)$ assists in describing the longitudinal safety distance constraint switching between the vehicles in two stages as a smooth transition process rather than sudden changes. Similarly, vehicles B and A also satisfy this similar change process. The change in the influence of vehicle B on vehicle A due to the change in vehicle M's cut-into is slightly different. Although vehicles B and A are still in the same lane in the LC-T stage, the longitudinal distance constraint is also changed to a negative value in this stage as vehicle M has become the actual preceding vehicle of vehicle A in this stage and the influence of vehicle B on vehicle A has been replaced by vehicle M.

The shape of $LPFB(*)$ is presented in Figure 5. This function also changes the lateral position of vehicle M, i.e., $y_M(k)$. In the LC-O stage, i.e., $0 \leq y_M(k) \leq d/2$, the value of the function $LPFB(*)$ increases with a slope of L_3 , i.e., $2/d$ from 0 to L_4 , i.e., 1. In the LC-T stage, the value of the function $LPFB(*)$ remains at L_4 , i.e., 1.

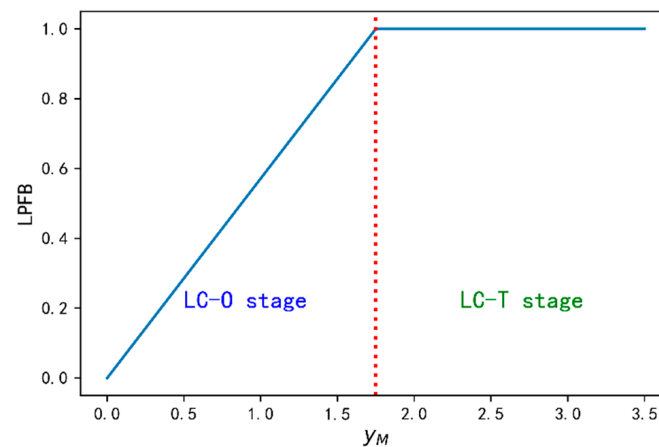


Figure 5. The trajectory curve of linear piecewise function $LPFB$.

Similar to $LPFA(*)$, $LPFB(*)$ also provides smooth longitudinal distance constraints switching processes between vehicles B and M and vehicles M and A. The difference is that with the help of the function $LPFB(*)$, the longitudinal distance constraint between vehicles B and M and vehicles M and A increases gradually in the LC-O stage. On the other hand, in the LC-T stage, the constraints remain constant after vehicles M and A enter the stable car-following mode.

(3) Comfort constraints

In order to guarantee a comfortable CLC, the accelerations of vehicles M and A should not be too large. Vehicles M and A have the same acceleration performance and satisfy the same upper and lower bounds of acceleration constraints.

$$a_{min} \leq a_M(k) \leq a_{max}, k = 1, 2, \dots, N-1 \quad (17)$$

$$a_{min} \leq a_A(k) \leq a_{max}, k = 1, 2, \dots, N-1 \quad (18)$$

where a_{min} and a_{max} denote the minimum and maximum comfortable acceleration acceptable for vehicles M and A. $a_M(k)$ and $a_A(k)$ represent the acceleration control inputs of vehicles M and A.

(4) Dynamic kinematics model constraints

The actual predictive models for vehicles M and A should be updated iteratively based on their differential longitudinal motion models, which are mathematically expressed as follows:

$$x_M(k+1) = x_M(k) + v_M(k)dt + a_M(k)dt^2/2, k = 1, 2, \dots, N-1 \quad (19)$$

$$v_M(k+1) = v_M(k) + a_M(k)dt, k = 1, 2, \dots, N-1 \quad (20)$$

$$x_A(k+1) = x_A(k) + v_A(k)dt + a_A(k)dt^2/2, k = 1, 2, \dots, N-1 \quad (21)$$

$$v_A(k+1) = v_A(k) + a_A(k)dt, k = 1, 2, \dots, N-1 \quad (22)$$

3.2.3. Objective Functions with Preceding Vehicle Switching of CLC Control Strategy

(1) Longitudinal distance tracking control with preceding vehicle switching

The longitudinal distance tracking error is described as the difference between the actual longitudinal distances between vehicles M, A, and their preceding vehicles and the expected longitudinal distance between these two vehicles. The expected longitudinal distance $d_{exp,M}(k)$ and $d_{exp,A}(k)$ are set according to the constant time headway rule.

$$d_{exp,M}(k) = v_M(k) * t_{hd} + d_0, k = 1, 2, \dots, N \quad (23)$$

$$d_{exp,A}(k) = v_A(k) * t_{hd} + d_0, k = 1, 2, \dots, N \quad (24)$$

In the LC-O stage, the longitudinal distance tracking errors between vehicles C and M, and B and A are computed using (25) and (26) as follows:

$$ex_{M1}(k) = S_{CM}(k) - d_{exp,M}(k), k = 1, 2, \dots, N \quad (25)$$

$$ex_{A1}(k) = S_{BA}(k) - d_{exp,A}(k), k = 1, 2, \dots, N \quad (26)$$

where t_{hd} denotes the expected time headway, which is a predetermined value.

In the LC-T stage, the longitudinal distance tracking errors between vehicles B and M, and M and A are calculated by using (27) and (28) as follows:

$$ex_{M2}(k) = S_{BM}(k) - d_{exp,M}(k), k = 1, 2, \dots, N \quad (27)$$

$$ex_{A2}(k) = S_{MA}(k) - d_{exp,A}(k), k = 1, 2, \dots, N \quad (28)$$

The preceding vehicle switching problem during the lane-changing process should be considered not only in the constraints but also in the optimization objectives. Based on the ideas of the previous longitudinal distance constraints construction between vehicles C and M, and B and A, the linear piecewise function $LPFB(*)$ is also applied to soften the change in the longitudinal distance tracking errors from the LC-O stage to LC-T stage when the preceding vehicle switches. It is evident from Figure 4 that this function can map the proportion of the switching of preceding vehicles to a range of $[0, 1]$, and take half of the total lateral distance $d/2$ as the watershed because of the two stages during the whole lane change. When the lateral distance is less than $d/2$, i.e., in the LC-O stage, the proportion coefficient gradually grows from 0 to 1 with a slope of $2/d$. On the contrary, when it is greater than $d/2$, i.e., in the LC-T stage, the proportion coefficient remains unchanged at 1.

Based on the aforementioned analysis, the longitudinal distance tracking errors of vehicles M and A are rewritten as (29) and (30). The linear piecewise function $LPFB(*)$ is used to control the weight values of the two preceding vehicles that should be switched and tracked.

$$\tilde{ex}_M(k) = LPFB(k)ex_{M2}(k) + [1 - LPFB(k)]ex_{M1}(k), k = 1, 2, \dots, N \quad (29)$$

$$\tilde{ex}_A(k) = LPFB(k)ex_{A2}(k) + [1 - LPFB(k)]ex_{A1}(k), k = 1, 2, \dots, N \quad (30)$$

where $\tilde{ex}_M(k)$ and $\tilde{ex}_A(k)$ represent the improved longitudinal distance tracking errors of vehicles M and its original and new preceding vehicles (i.e., vehicles C and B), and vehicles A and its original and new preceding vehicles (i.e., vehicles B and M), respectively.

(2) Longitudinal speed tracking control with preceding vehicle switching

In addition, vehicles M and A should track their expected longitudinal distances while tracking the longitudinal speeds of their preceding vehicles during the process of lane change. Therefore, longitudinal speed-tracking errors should also be considered.

In the LC-O stage, the longitudinal speed tracking errors between vehicles C and M, and B and A are expressed as (31) and (32).

$$ev_{M1}(k) = v_M(k) - v_C(k), k = 1, 2, \dots, N \quad (31)$$

$$ev_{A1}(k) = v_A(k) - v_B(k), k = 1, 2, \dots, N \quad (32)$$

In the LC-T stage, the longitudinal speed tracking errors between vehicles B and M, and M and A are expressed by using (33) and (34).

$$ev_{M2}(k) = v_M(k) - v_B(k), k = 1, 2, \dots, N \quad (33)$$

$$ev_{A2}(k) = v_A(k) - v_M(k), k = 1, 2, \dots, N \quad (34)$$

Similar to the longitudinal distance tracking errors associated with vehicles M and A, the condition of the preceding vehicles switching should be considered in longitudinal speed tracking errors as presented in (35) and (36).

$$\tilde{e}v_M(k) = LPFB(k)ev_{M2}(k) + [1 - LPFB(k)]ev_{M1}(k), k = 1, 2, \dots, N \quad (35)$$

$$\tilde{e}v_A(k) = LPFB(k)ev_{A2}(k) + [1 - LPFB(k)]ev_{A1}(k), k = 1, 2, \dots, N \quad (36)$$

where $\tilde{e}v_M(k)$ and $\tilde{e}v_A(k)$ represent the improved longitudinal speed tracking errors of vehicles M and B, C, and vehicles A and B, M, respectively.

(3) Comfort

Acceleration is an important indicator of driving comfort. An acceleration with small fluctuations leads to a better driving experience. Thus, considering the comfort of the vehicles, we need to constraint the control quantities like $a_M(k)$ and $a_A(k)$.

Furthermore, jerk is another important factor that influences ride comfort. In order to improve the ride comfort, the jerk values of all the vehicles should be as small as possible [43]. All jerk values in this work are expressed based on the variations of the control quantities within a single step and are mathematically expressed in (37) and (38).

$$j_M(k) = [a_M(k+1) - a_M(k)]/dt, k = 1, 2, \dots, N-2 \quad (37)$$

$$j_A(k) = [a_A(k+1) - a_A(k)]/dt, k = 1, 2, \dots, N-2 \quad (38)$$

where $j_M(k)$ and $j_A(k)$ represent the jerk values of longitudinal motion control of vehicles M and A.

(4) Objective function of the optimization model

In summary, we obtain the following objective function of the optimization model based on MPC:

$$\begin{aligned} \min J(s) = \sum_{k=1}^N & \left[\omega_{ex_M} \|\tilde{e}x_M(s+k)\|^2 + \omega_{ev_M} \|\tilde{e}v_M(s+k)\|^2 \right. \\ & \left. + \omega_{ex_A} \|\tilde{e}x_A(s+k)\|^2 + \omega_{ev_A} \|\tilde{e}v_A(s+k)\|^2 \right] \\ & + \sum_{k=1}^{N-1} \left[\omega_{a_M} \|a_M(s+k)\|^2 + \omega_{a_A} \|a_A(s+k)\|^2 \right] \\ & + \sum_{k=1}^{N-2} \left[\omega_{j_M} \|j_M(s+k)\|^2 + \omega_{j_A} \|j_A(s+k)\|^2 \right] \end{aligned} \quad (39)$$

where $J(s)$ represents the sum of comfort, tracking, and traffic efficiency cost of the optimization model. A discrete time interval is set as dt . N represents the length of the predictive horizon. ω_{ex_M} , ω_{ev_M} , ω_{ex_A} , ω_{ev_A} , ω_{a_M} , ω_{a_A} , ω_{j_M} , and represent the weighting factor of each item. $(s+k)$ denotes the predicted state at time $s+k$, and s denotes the current time.

In the first summarization term presented in (39), the first two items represent the penalty for the longitudinal tracking error of vehicle M considering the switching of the preceding vehicles. The last two items represent the penalty for the longitudinal tracking error of vehicle A considering the preceding vehicles switching.

In the second summarization term presented in (39), the two items represent the penalties for vehicles M and A's expected control accelerations.

In the last summarization term presented in (39), the two items represent the penalties for the jerks of vehicles M and A, respectively.

All the constraints of the optimization model are summarized as follows:

$$\left\{ \begin{array}{l} x_M(s+k+1) = x_M(s+k) + v_M(s+k)dt + a_M(s+k)dt^2/2, k = 1, 2, \dots, N-1 \\ v_M(s+k+1) = v_M(s+k) + a_M(s+k)dt, k = 1, 2, \dots, N-1 \\ x_A(s+k+1) = x_A(s+k) + v_A(s+k)dt + a_A(s+k)dt^2/2, k = 1, 2, \dots, N-1 \\ v_A(s+k+1) = v_A(s+k) + a_A(s+k)dt, k = 1, 2, \dots, N-1 \\ S_{CM}(s+k) \geq S_{safe,CM}(s+k)LPFA(s+k), k = 1, 2, \dots, N \\ S_{BM}(s+k) \geq S_{safe,BM}(s+k)LPFB(s+k), k = 1, 2, \dots, N \\ S_{BA}(s+k) \geq S_{safe,BA}(s+k)LPFA(s+k), k = 1, 2, \dots, N \\ S_{MA}(s+k) \geq S_{safe,MA}(s+k)LPFB(s+k), k = 1, 2, \dots, N \\ 0 < v_M(s+k) \leq \begin{cases} v_{Omax} & \text{if } 0 \leq y_M(s+k) \leq d/2 \\ v_{Tmax} & \text{otherwise} \end{cases}, k = 1, 2, \dots, N \\ 0 < v_A(s+k) \leq v_{Tmax}, k = 1, 2, \dots, N \\ a_{min} \leq a_M(s+k) \leq a_{max}, k = 1, 2, \dots, N-1 \\ a_{min} \leq a_A(s+k) \leq a_{max}, k = 1, 2, \dots, N-1 \end{array} \right. \quad (40)$$

Since the vehicle motion state prediction model used in this study is a classical linear vehicle kinematic model, the online optimization problem of the MPC controller based on this model is a nonlinear, convex optimization problem (its constraint function is also composed of a series of linear expressions). Therefore, a suitable rolling time domain optimization tool can be used to optimize and iterate the deviation amount within a finite rolling time interval. Here, the discrete nonlinear optimization problem presented in (39) and (40) in the receding horizon can be solved with the help of the advanced optimization solver pyomo in Python [44]. The state quantities at time s are used as the state values of the first step for performing N -step prediction, i.e., $*(s+1)$ equals $*(s)$. By solving this model predictive optimization problem, the desired control inputs of the two vehicles in each control period are obtained and active cooperation can be implemented according to the desired control inputs. Please note that a control sequence containing $N-1$ control variables can be gained by solving the model predictive optimization problem. However, only the first element of the control sequence is selected as the final desired control input.

3.3. Solvability Analysis of the Proposed CLC Control Strategy

MPC-based control strategies should be online feasible, and sequential solvability is one way to measure online feasibility. Specifically, it means the optimization problem (39) and (40) can find a feasible solution at each step if their initial states are feasible. The constraints in (39) and (40) consider two perspectives: safety and comfort. The following analysis proves that if the longitudinal safety distance constraints of controlled vehicles and their preceding vehicles are satisfied at the k step, we can always find a solution that satisfies the constraints of comfort to make the longitudinal safety distance constraints hold at the $k+1$ step. Due to the different preceding vehicle switching functions and safety constraints designed in different lane change stages, we will first investigate the vehicles C and M, and vehicles B and A adopting the same preceding vehicle switching function $LPFA(*)$ (i.e., At the LC-O stage) from Lemma 1 to Lemma 2. Then, the vehicles B and M, and vehicles M and A (i.e., at the LC-T stage) adopting the same preceding vehicle switching function $LPFB(*)$ will be investigated from Lemma 3 to Lemma 4. Note that the mathematical method for analyzing the sequential solvability of each controlled vehicle and its preceding vehicle are similar. However, due to the difference in the constraints' mathematical format (such as preceding vehicle switching function $LPFA(*)$ and $LPFB(*)$), the investigation processes will be present one by one as each controlled vehicle and its preceding vehicle in two stages.

Lemma 1. Given $S_{CM}(k) \geq S_{safe,CM}(k)LPFA(k)$ is satisfied at step, a feasible solution $a_M(k) = a_{min}$ can make $S_{CM}(k+1) \geq S_{safe,CM}(k+1)LPFA(k+1)$ hold, if the speed difference between vehicles C and M satisfies $v_C(k) - v_M(k) \geq a_{min}dt/2$ for any step ($k = 1, 2, \dots, N$).

Proof. Since $LPFA(*)$ is a segmented function, it needs to be discussed separately. When $0 \leq y_M(k) \leq d/2$ and because all critical longitudinal safety distances is a fixed value d_0 , the following relationship exists.

$$S_{CM}(k) \geq S_{safe,CM}(k)LPFA(k) = d_0L_1 \quad (41)$$

The above Equation (41) can be rewritten in the following form.

$$S_{CM}(k) - S_{safe,CM}(k)LPFA(k) = S_{CM}(k) - d_0L_1 \geq 0 \quad (42)$$

By substituting (4) into (42), the following inequality (43) can be obtained.

$$\begin{aligned} S_{CM}(k+1) - S_{safe,CM}(k+1)LPFA(k+1) &= S_{CM}(k+1) - d_0L_1 \\ &= S_{CM}(k) + [v_C(k) - v_M(k)]dt - a_M(k)dt^2/2 - d_0L_1 \\ &\geq [v_C(k) - v_M(k)]dt - a_M(k)dt^2/2 \end{aligned} \quad (43)$$

Let $a_M(k) = a_{min}$ and if the speed difference between vehicles C and M satisfies $v_C(k) - v_M(k) \geq a_{min}dt/2$ at the same time, the following inequality (44) will be held after multi-step amplification.

$$\begin{aligned} S_{CM}(k+1) - S_{safe,CM}(k+1)LPFA(k+1) \\ &\geq [v_C(k) - v_M(k)]dt - a_M(k)dt^2/2 \\ &= a_{min}dt^2/2 - a_{min}dt^2/2 = 0 \end{aligned} \quad (44)$$

Thus, when $0 \leq y_M(k) \leq d/2$, the longitudinal distance constraint $S_{CM}(k+1) \geq S_{safe,CM}(k+1)LPFA(k+1)$ will be satisfied at $k+1$ step.

When $y_M(k) > d/2$, the following relationship exists.

$$S_{CM}(k) \geq S_{safe,CM}(k)LPFA(k) = d_0LPFA(k) \quad (45)$$

Equation (45) can also be rewritten as following; Equation (46).

$$S_{CM}(k) - S_{safe,CM}(k)LPFA(k) = S_{CM}(k) - d_0LPFA(k) \geq 0 \quad (46)$$

When $y_M(k) > d/2$, the function $LPFA(*)$ is monotonically decreasing, so we have $LPFA(k+1) < LPFA(k)$, then by substituting (4) and (46), the following inequality (47) can be obtained.

$$\begin{aligned} S_{CM}(k+1) - S_{safe,CM}(k+1)LPFA(k+1) &= S_{CM}(k+1) - d_0LPFA(k+1) \\ &> S_{CM}(k+1) - d_0LPFA(k) \\ &= S_{CM}(k) + [v_C(k) - v_M(k)]dt - a_M(k)dt^2/2 - d_0LPFA(k) \\ &\geq [v_C(k) - v_M(k)]dt - a_M(k)dt^2/2 \end{aligned} \quad (47)$$

Let $a_M(k) = a_{min}$, and if the speed difference between vehicles C and M satisfies $v_C(k) - v_M(k) \geq a_{min}dt/2$ at the same time, the following inequality will be held after multi-step amplification.

$$\begin{aligned} S_{CM}(k+1) - S_{safe,CM}(k+1)LPFA(k+1) \\ &\geq [v_C(k) - v_M(k)]dt - a_M(k)dt^2/2 = 0 \end{aligned} \quad (48)$$

Hence, when $y_M(k) > d/2$, the longitudinal distance constraint $S_{CM}(k+1) \geq S_{safe,CM}(k+1)LPFA(k+1)$ will be satisfied at $k+1$ step.

To sum up, the analysis, if $v_C(k) - v_M(k) \geq a_{min}dt/2$ is satisfied, $S_{CM}(k+1) \geq S_{safe,CM}(k+1)LPFA(k+1)$ will hold, given that $S_{CM}(k) \geq S_{safe,CM}(k)LPFA(k)$. The proof of Lemma 1 is closed. \square

Lemma 2. Given $S_{BA}(k) \geq S_{safe,BA}(k)LPFA(k)$ is satisfied at k step, a feasible solution $a_A(k) = a_{min}$ can make $S_{BA}(k+1) \geq S_{safe,BA}(k+1)LPFA(k+1)$ hold, if the speed difference between vehicles B and A satisfies $v_B(k) - v_A(k) \geq a_{min}dt/2$ for any step k ($k = 1, 2, \dots, N$).

Proof. The proof process of lemma 2 is similar to that of Lemma 1 and will not be repeated here. \square

Lemma 3. Given $S_{BM}(k) \geq S_{safe,BM}(k)LPFB(k)$ is satisfied at k step, a feasible solution $a_M(k) = a_{min}$ can make $S_{BM}(k+1) \geq S_{safe,BM}(k+1)LPFB(k+1)$ hold, if the speed difference between vehicles B and M satisfies $v_B(k) - v_M(k) \geq a_{min}dt/2 + d_0L_3\Delta y_{M_{min}}$ for any step k ($k = 1, 2, \dots, N$).

Proof. Since $LPFB(*)$ is also a segmented function, it needs to be discussed separately. When $0 \leq y_M(k) \leq d/2$, the following relationship exists.

$$S_{BM}(k) \geq S_{safe,BM}(k)LPFB(k) = d_0L_3y_M(k) \quad (49)$$

Equation (49) can be rewritten in the following form.

$$S_{BM}(k) - S_{safe,BM}(k)LPFB(k) = S_{BM}(k) - d_0L_3y_M(k) \geq 0 \quad (50)$$

According to the mathematical expression of $LPFB(*)$, the following Equation (51) can be obtained:

$$S_{safe,BM}(k+1)LPFB(k+1) = d_0L_3y_M(k+1) = d_0L_3[y_M(k) + \Delta y_M(k)] \quad (51)$$

By substituting (4) and (51), the following Equation (52) can be obtained.

$$\begin{aligned} S_{BM}(k+1) - S_{safe,BM}(k+1)LPFB(k+1) &= S_{BM}(k+1) - d_0L_3[y_M(k) + \Delta y_M(k)] \\ &= S_{BM}(k) + [v_B(k) - v_M(k)]dt - a_M(k)dt^2/2 \\ &\quad - d_0L_3[y_M(k) + \Delta y_M(k)] \\ &\geq [v_B(k) - v_M(k)]dt - a_M(k)dt^2/2 - d_0L_3\Delta y_M(k) \end{aligned} \quad (52)$$

Let $a_M(k) = a_{min}$ and $\Delta y_M(k) = \Delta y_{M_{min}}$, where $\Delta y_{M_{min}}$ is the minimal single-step lateral movement distance, and if the speed difference between vehicles B and M satisfies $v_B(k) - v_M(k) \geq a_{min}dt/2 + d_0L_3\Delta y_{M_{min}}$ at the same time, the following inequality (53) will be held after the multi-step amplification.

$$\begin{aligned} S_{BM}(k+1) - S_{safe,BM}(k+1)LPFB(k+1) &\geq [v_B(k) - v_M(k)]dt - a_M(k)dt^2/2 - d_0L_3\Delta y_M(k) \\ &= a_{min}dt^2/2 + d_0L_3\Delta y_{M_{min}} - a_{min}dt^2/2 - d_0L_3\Delta y_{M_{min}} = 0 \end{aligned} \quad (53)$$

Thus, when $0 \leq y_M(k) \leq d/2$, the longitudinal distance constraint $S_{BM}(k+1) \geq S_{safe,BM}(k+1)LPFB(k+1)$ will be satisfied at $k+1$ step.

When $y_M(k) > d/2$, the following relationship exists.

$$S_{BM}(k) \geq S_{safe,BM}(k)LPFB(k) = d_0L_4 \quad (54)$$

Equation (54) also can be rewritten as following Equation (55).

$$S_{BM}(k) - S_{safe,BM}(k)LPFB(k) = S_{BM}(k) - d_0L_4 \geq 0 \quad (55)$$

When $y_M(k) > d/2$, by substituting (4) and (55), the following inequality (56) can be obtained.

$$\begin{aligned} S_{BM}(k+1) - S_{safe,BM}(k+1)LPFB(k+1) &= S_{BM}(k+1) - d_0L_4 \\ &= S_{BM}(k) + [v_B(k) - v_M(k)]dt - a_M(k)dt^2/2 - d_0L_4 \\ &\geq [v_B(k) - v_M(k)]dt - a_M(k)dt^2/2 \end{aligned} \quad (56)$$

Let $a_M(k) = a_{min}$, and if the speed difference between vehicles B and M satisfies $v_B(k) - v_M(k) \geq a_{min}dt/2$ at the same time, the following inequality will be held after multi-step amplification.

$$\begin{aligned} S_{BM}(k+1) - S_{safe,BM}(k+1)LPFB(k+1) \\ \geq [v_B(k) - v_M(k)]dt - a_M(k)dt^2/2 = 0 \end{aligned} \quad (57)$$

Hence, when $y_M(k) > d/2$, the longitudinal distance constraint $S_{BM}(k+1) \geq S_{safe,BM}(k+1)LPFB(k+1)$ will be satisfied at $k+1$ step.

To sum up, the above analysis, if $v_B(k) - v_M(k) \geq a_{min}dt/2 + d_0L_3\Delta y_{M_{min}}$ is satisfied, $S_{BM}(k+1) \geq S_{safe,BM}(k+1)LPFB(k+1)$ will hold, given that $S_{BM}(k) \geq S_{safe,BM}(k)LPFB(k)$. The proof of Lemma 3 is closed. \square

Lemma 4. Given $S_{MA}(k) \geq S_{safe,MA}(k)LPFB(k)$ is satisfied at k step, a feasible solution $a_M(k) = a_{max}$ and $a_A(k) = a_{min}$ can make $S_{MA}(k+1) \geq S_{safe,MA}(k+1)LPFB(k+1)$ hold, if the speed difference between vehicles M and A satisfies $v_M(k) - v_A(k) \geq (a_{min} - a_{max})dt/2 + d_0L_3\Delta y_{M_{min}}$ for any step k ($k = 1, 2, \dots, N$).

Proof. The proof process of lemma 4 is similar to that of Lemma 3 and will not be repeated here. \square

In summary, vehicle differences between the controlled vehicles (A and D) and their preceding vehicles in the LC-O and LC-T stages are provided as the Lemma 1 to Lemma 4 to ensure the sequential solvability of the optimization problem (39) and (40) in the proposed CLC control strategy.

It should be noted that the above conclusion is based on the longitudinal distances among vehicles close to the critical longitudinal safety distance d_0 , if the longitudinal distance between the controlled vehicle and its preceding vehicle is greater than this critical value, then the speed difference between the controlled vehicle and its preceding vehicle is allowed to have a greater lower limit.

4. Numerical Simulations

4.1. Experiments Design and Parameter Settings

In order to verify the feasibility and practicability of the proposed strategy, two typical preset lane change scenarios are selected to conduct the experiments. In order to intuitively evaluate the control effects of the proposed control strategy, we first compare the motion trajectory and control input diagrams of the proposed CLC control strategy and the combined CACC and sine function (CACC_Sine) control strategy. The latter also adopts the lane change longitudinal-lateral independent analysis. Then the statistical indicators of the difference between the actual and the expected motion states of the two control strategies are presented to validate the improvement effect of the proposed CLC control strategy for ensuring the stability of traffic flow in the target lane after changing lanes.

The parameters of the proposed model are presented in Table 1. For the weighting parameters, we select different weight coefficients depending on the importance of different terms in the optimization problem to ensure that the final optimization results meet the control requirements. Specifically, in the tuning process, we first determine the weight coefficients of the spacing and speed tracking errors (i.e., $\tilde{e}x_M$, $\tilde{e}x_A$, $\tilde{e}v_M$, and $\tilde{e}v_A$), and in this study, we consider that the spacing and speed tracking errors of the lane change vehicle M and the cooperative vehicle A are of the same importance, so we set these weight

coefficients to the same value, i.e., $\omega_{ex_M} = \omega_{ex_A} = \omega_{ev_M} = \omega_{ev_A}$. After determining the weight coefficients of the spacing and speed tracking errors, we keep them unchanged and then adjust the weight coefficients of the control accelerations (i.e., a_M and a_A) and control jerks (i.e., j_M and j_A). In this study, considering the driving comfort, the accelerations and jerks of the controlled vehicles M and A should be ensured to be as small as possible, so the weight coefficients of the control accelerations and jerks are chosen to be larger than those of the spacing and speed tracking errors in this study. In addition, during the experiment, we found that too large control accelerations weight coefficients will prolong the time for the controlled vehicles to reach the desired motion states, so the control accelerations weight coefficients are higher than the spacing and speed tracking errors weight coefficients and smaller than the jerks weight coefficients in this experiment, that is $\omega_{ex_M} = \omega_{ex_A} = \omega_{ev_M} = \omega_{ev_A} < \omega_{a_M} = \omega_{a_A} < \omega_{j_M} = \omega_{j_A}$.

Table 1. Related parameters in the simulations.

Related Parameters	Value	Related Parameters	Value
T	4 s	d	3.5 m
v_{Omax}	20 m/s	v_{Tmax}	30 m/s
d_0	5 m	L_1	1
L_2	−1000	L_3	0.571
L_4	1	a_{min}	−4 m/s ²
a_{max}	2 m/s ²	dt	0.1 s
ω_{ex_M}	200	ω_{ev_M}	200
ω_{ex_A}	200	ω_{ev_A}	200
ω_{a_M}	500	ω_{a_A}	500
ω_{j_M}	1000	ω_{j_A}	1000
t_{hd}	1.2 s		

In these two comparative experiments, the CACC model for the longitudinal movement of the lane change adopts the CACC car-following model with constant time headway proposed in [45]. The lateral movement is described by the sine function, which is the same as the proposed CLC control strategy. Please note that there is no cooperation between all the controlled CAVs in this comparative control strategy. Therefore, vehicles M and A keep track of vehicles C and B during the LC-O phase and do not track vehicles B and M until the LC-T phase, and it is considered that their preceding vehicles suddenly change from the LC-O stage to LC-T stage.

The selection of lane-changing time has a great influence on the security of the actual lane change on the highway. The statistical analysis shows that a vehicle generally takes 3–5 s to complete the accelerated lane-changing process. The longer time the vehicle takes, the more dangerous is the process [46]. Therefore, the duration of lane-changing process in the sine function is set as 4 s.

The simulations are conducted on a two-lane road segment developed in Python. Two representative lane-changing scenarios are selected. First, a general lane-changing scenario, where the longitudinal distance between vehicles B and A in the target lane is large enough to provide a safe lane-changing gap without requiring a significant speed adjustment by vehicle A. Second, the longitudinal distance between vehicles B and A in the target lane is relatively smaller, which requires vehicle A to make active speed adjustment to provide a safe lane change gap. The specific scene parameters at the beginning of the lane-changing process are presented below:

Scenario 1: $v_M(0) = 17$ m/s, $v_B(0) = 22$ m/s, $v_C(0) = 18$ m/s, $v_A(0) = 20$ m/s, $S_{CM}(0) = 18$ m, $S_{BM}(0) = 15$ m, $S_{MA}(0) = 22$ m;

Scenario 2: $v_M(0) = 18$ m/s, $v_B(0) = 20$ m/s, $v_C(0) = 18$ m/s, $v_A(0) = 19$ m/s, $S_{CM}(0) = 10$ m, $S_{BM}(0) = 15$ m, $S_{MA}(0) = 10$ m.

We compare the control effects of the proposed model and the comparative model including the LC-O stage and LC-T stage, and select the same experimental duration, which is 30 s for scenarios 1 and 2.

4.2. Performance Comparison of the Proposed CLC Control Strategy and Combination with CACC and Sine Function Control Strategy

Figures 6 and 7 show the longitudinal position and speed variations of vehicles M, A, and B of two control strategies in scenario 1. Considering the longitudinal positions, as shown in Figure 6a, the proposed CLC control strategy realizes smooth switching of vehicle A's tracking-preceding vehicles from vehicles B to M. It also makes the vehicles on the target lane (i.e., vehicles B, M, and A) quickly attain stable car-following states in the LC-T stage and keeps longitudinal safety distances among vehicles B, M, and A from the initial instant of the LC-T stage. As presented in Figure 6b, for the comparative CACC_Sine control strategy, vehicle A in the LC-O stage regards vehicle B as its tracking-preceding vehicle. Therefore, in the LC-O stage, vehicle A gradually approaches vehicle B longitudinally in the LC-T stage, and vehicle A takes vehicle M as its new preceding vehicle. Eventually, during the transition from the LC-O stage to the LC-T stage, the longitudinal distance between the vehicles M and A is slightly higher as compared to the basic safety distance requirement, i.e., 5 m.

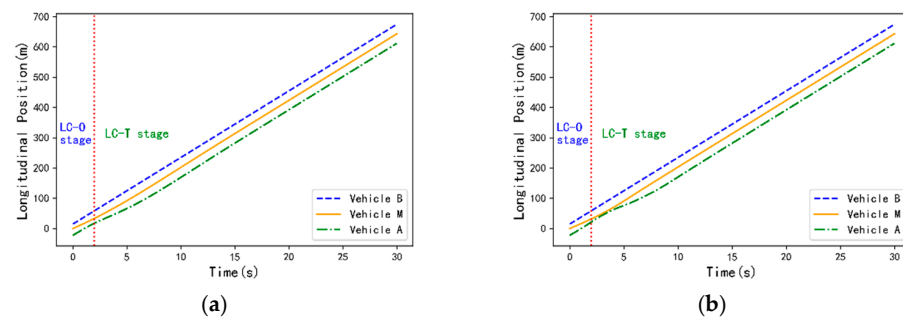


Figure 6. The longitudinal positions of vehicles B, M, and A of the two control strategies in scenario 1. (a) The proposed CLC control strategy, (b) CACC_Sine control strategy.

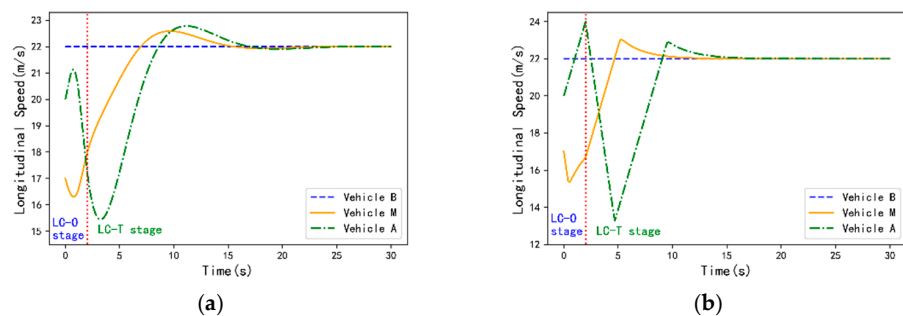


Figure 7. The longitudinal speeds of vehicles B, M and A of the two control strategies in scenario 1. (a) The proposed CLC control strategy, (b) CACC_Sine control strategy.

Considering the longitudinal speeds, Figure 7 shows that the proposed CLC control strategy has smoother speed variation and less fluctuations as compared to the CACC_Sine control strategy. Furthermore, the proposed CLC control strategy considering the preceding vehicle switching avoids excessive speed adjustment in the LC-O stage, thus enabling a smooth speed transition from the LC-O stage to the LC-T stage (Figure 7a), instead of the more drastic speed change of the CACC_Sine strategy (Figure 7b). Moreover, the speed variation trends of the two control strategies show that the trajectory of vehicle A follows the trend of vehicle B from 5 s in the proposed CLC strategy, while in the CACC_Sine control strategy vehicle A follows from 10 s with an obvious sequential change. As an optimal controller, the proposed CLC control strategy obtains the optimal control quantities based

on the current motion state of all related vehicles, while CACC_Sine is an independent control structure and is non-optimal for the following vehicle's control quantity, which only relies on its preceding vehicle.

Figure 8 shows the actual and expected longitudinal distances between vehicles M and A and their preceding vehicles of two control strategies in scenario 1. In the LC-O stage, it is evident that the CACC_Sine control strategy has a better tracking control effect as compared to the proposed CLC control strategy, because it considers that the tracking-preceding vehicles of controlled vehicles doesn't change in this stage. However, for vehicle A, it is unable to provide a sufficient gap for vehicle M to cut into the lane when its preceding vehicle suddenly switches to vehicle M. Due to the consideration of preceding vehicle switching in the proposed CLC control strategy, vehicle A is far away from its expected distance in the late period of the LC-O stage to make preparation for vehicle M's merging. In the LC-T stage, as compared with the CACC_Sine control strategy, the proposed CLC control strategy has a better tracking control effect for vehicle A, while having a relatively larger tracking control error in the early LC-T stage, i.e., from 3 s to 10 s. However, it can reach the expected tracking state at about 20 s which is the same as CACC_Sine control strategy.

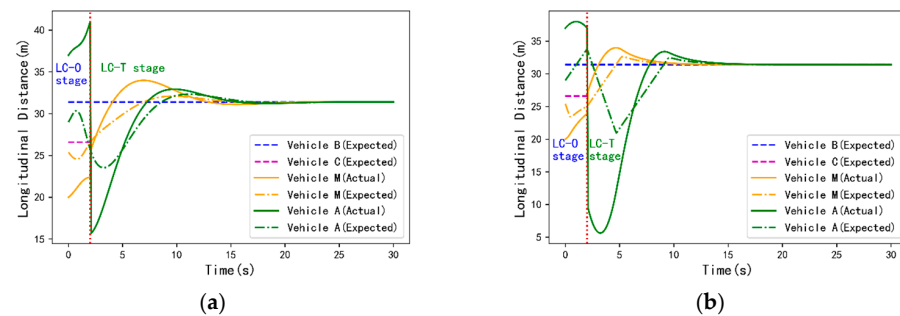


Figure 8. The actual and expected longitudinal distances between vehicles M, A and their preceding vehicles in two stages of the two control strategies in scenario 1. (a) The proposed CLC control strategy, (b) CACC_Sine control strategy.

Figures 9 and 10 show the comparison between the longitudinal accelerations and jerks for the proposed CLC control strategy and the comparative CACC_Sine control strategy. The acceleration and jerk of the proposed CLC control strategy are more continuous. However, the CACC_Sine control strategy shows sharp variations with extreme fluctuations. According to Figure 10, it is easy to observe that the longitudinal jerk of the proposed CLC control strategy fluctuates within a low range, i.e., from -0.8 m/s^3 to 0.4 m/s^3 . However, the longitudinal jerk of the CACC_Sine control strategy fluctuates more frequently and with greater amplitude, i.e., greater than 4 m/s^3 , which causes a significant driving discomfort. As a result, the proposed CLC control strategy has smoother acceleration and less fluctuating jerk compared to the comparative CACC_Sine control strategy, thus ensuring driving comfort and leading to a better driving experience.

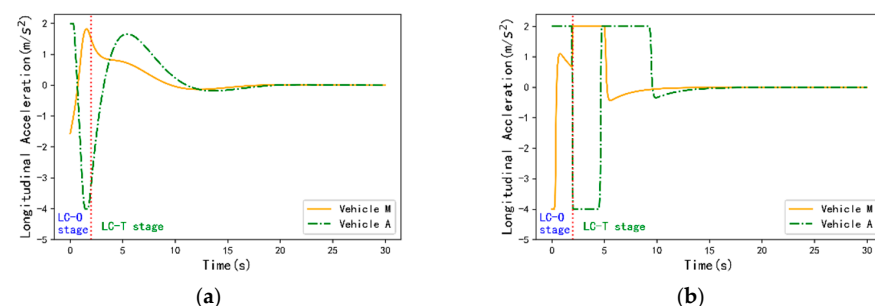


Figure 9. The longitudinal accelerations of vehicles M and A of the two control strategies in scenario 1. (a) The proposed CLC control strategy, (b) CACC_Sine control strategy.

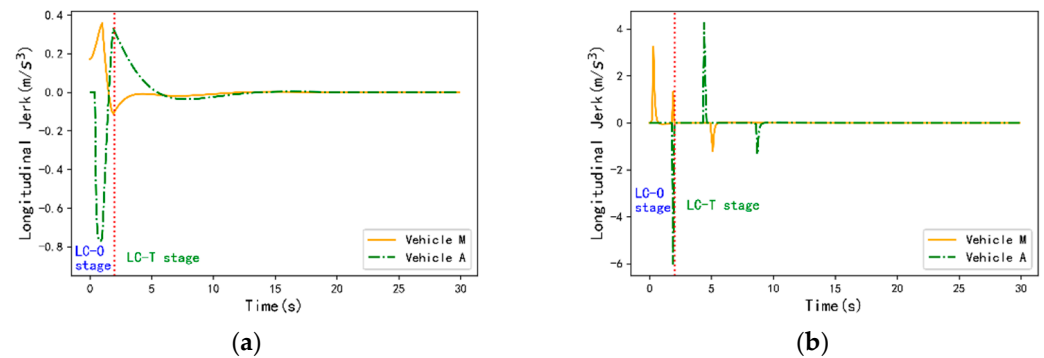


Figure 10. The longitudinal jerks of vehicles M and A of the two control strategies in scenario 1. (a) The proposed CLC control strategy, (b) CACC_Sine control strategy.

Similarly, Figures 11–15 show the longitudinal positions and speeds of vehicles M, A, and B, and the longitudinal distances between vehicles M, A, and their preceding vehicles and longitudinal accelerations and jerks of vehicles M and A of two control strategies with the change of time for another typical lane change scenario. As compared with scenario 1, in scenario 2, the vehicles M and A in scenario 2 are closer longitudinally and the speed differences between vehicle M and vehicles B and A are smaller. Figures 11–13 show that when the longitudinal distance between vehicles on the target lane is unable to meet the safe lane-changing gap, the proposed CLC control strategy smoothly completes the preceding vehicle switching and actively changes the speed of vehicle A in the LC-O stage to ensure the safety of vehicle M when entering the target lane in the LC-T stage. Based on this smooth switching method, a more continuous speed profile can be obtained, which can produce a leading effect on the upstream traffic flow. However, for the CACC_Sine control strategy without the consideration of preceding vehicle switching, the longitudinal distance between vehicles M and A at the beginning of the LC-T stage, i.e., from 2 s to 5 s, is very slightly greater than 0 with a great risk of collision. As a result, vehicles M and A should make a greater speed adjustment as compared to the proposed CLC control strategy to ensure safety and catch up with their preceding vehicles quickly. Figures 14 and 15 also show that the acceleration and jerk of the CACC_Sine control strategy are more volatile as compared to the proposed CLC control strategy, which means that the proposed CLC control strategy has better performance in terms of ensuring driving comfort.

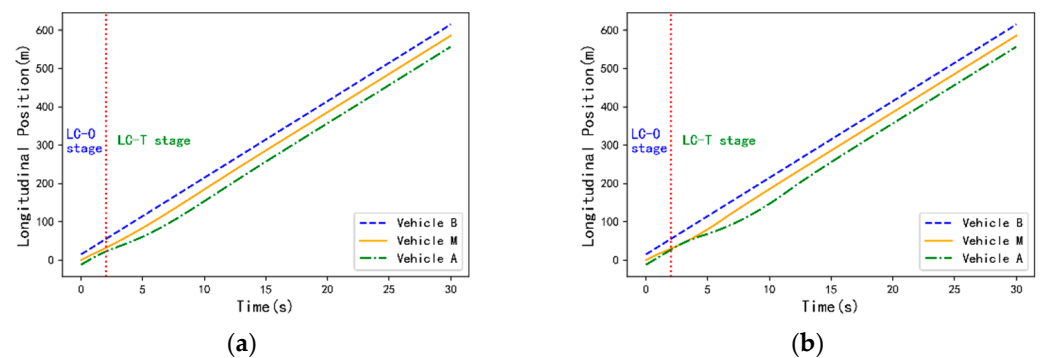


Figure 11. The longitudinal positions of vehicles B, M, and A of the two control strategies in scenario 2. (a) The proposed CLC control strategy, (b) CACC_Sine control strategy.

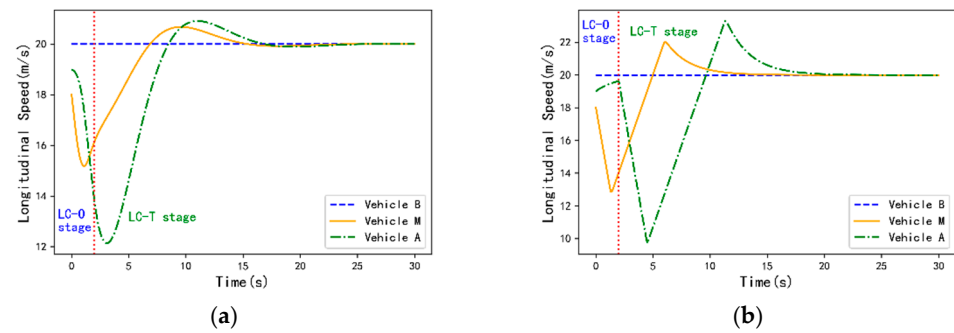


Figure 12. The longitudinal speeds of vehicles B, M and A of the two control strategies in scenario 2. (a) The proposed CLC control strategy, (b) CACC_Sine control strategy.

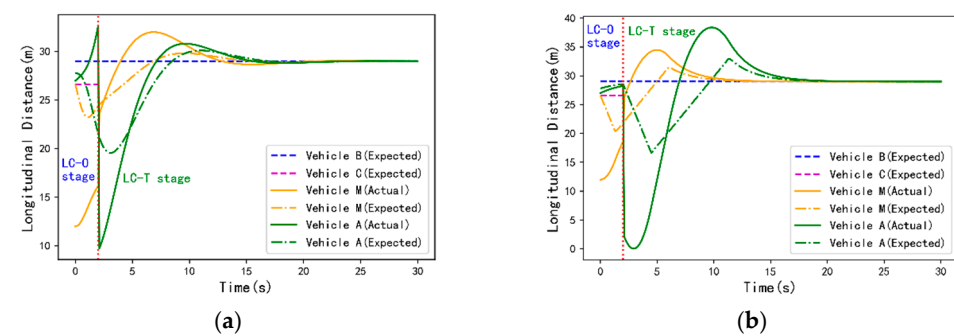


Figure 13. The Actual and Expected longitudinal distances between vehicles M, A and their preceding vehicles in two stages of the two control strategies in scenario 2. (a) The proposed CLC control strategy, (b) CACC_Sine control strategy.

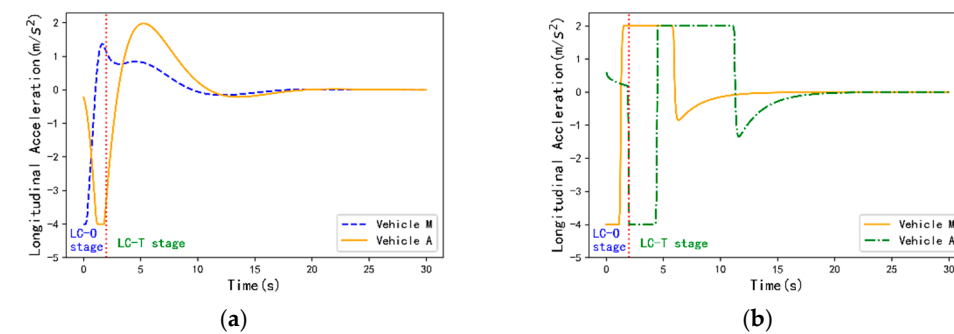


Figure 14. The longitudinal accelerations of vehicles M and A of the two control strategies in scenario 2. (a) The proposed CLC control strategy, (b) CACC_Sine control strategy.

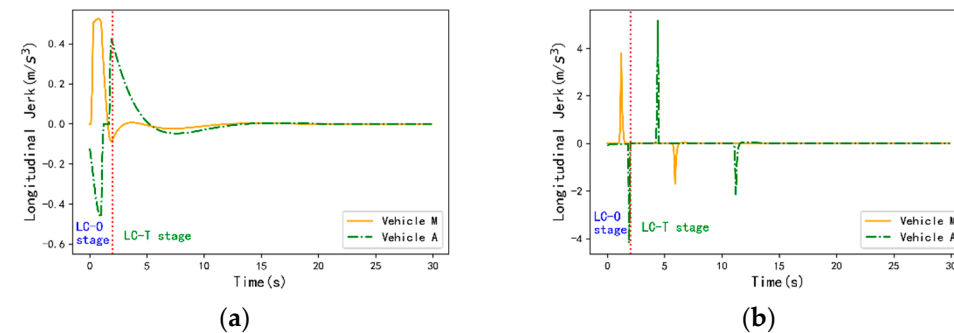


Figure 15. The longitudinal jerks of vehicles M and A of the two control strategies in scenario 2. (a) The proposed CLC control strategy, (b) CACC_Sine control strategy.

In summary, the proposed CLC control strategy achieves smooth preceding vehicle switching of the controlled vehicles M and A during the lane-changing process. Please note that the smoother speed variations have a positive impact on traffic flow upstream of the target lane, this improving road mobility. In addition, less fluctuating acceleration and jerk effectively ensure the driving comfort.

In order to analyze the improvement effect of the proposed CLC control strategy on the traffic flow of the target lane, some statistical indicators of the difference between the actual and expected motion states in the LC-T stage are analyzed for the above two lane-changing scenarios. Tables 2 and 3 show the statistical indicators of the difference between the actual and expected longitudinal distances and speeds of vehicles M, A, and their preceding vehicles in the LC-T stage for the two control strategies in two scenarios, respectively. The first three characters “Avg”, “Std”, and “Max” in all the indicators of all tables denote the average, standard deviation, and maximum, respectively. The last five characters “DLD_M(A)” and “DLS_M(A)” in Tables 2 and 3 denote the difference between the actual and the expected longitudinal distances and speeds of the vehicle M (A) and its preceding vehicle. It is evident that most of the indicators in the proposed CLC control strategy for longitudinal distance and speed tracking effects are obviously below that of the CACC_Sine control strategy. Although the average indicator of longitudinal distance tracking of the proposed CLC control strategy in scenario 1 is slightly better as compared to the CACC_Sine control strategy, its standard deviation and maximum are still better. It shows that the proposed CLC control strategy has better tracking control effects of vehicles M and A in the target lane during the LC-T stage and ensures a more stable car-following state.

Table 2. Indicator comparison for longitudinal distance of two control strategies.

Control Strategies Indicators	Scenario 1		Scenario 2	
	CLC	CACC_Sine	CLC	CACC_Sine
AvgDLD_M (m)	0.630	0.432	0.718	0.928
StdDLD_M (m)	0.952	1.029	1.091	1.972
MaxDLD_M (m)	3.053	4.023	3.510	6.918
AvgDLD_A (m)	0.733	2.487	0.835	3.748
StdDLD_A (m)	1.649	6.048	1.896	6.404
MaxDLD_A (m)	10.121	24.229	12.069	25.978

Table 3. Indicator comparison for longitudinal speed of two control strategies.

Control Strategies Indicators	Scenario 1		Scenario 2	
	CLC	CACC_Sine	CLC	CACC_Sine
AvgLSD_M (m/s)	0.428	0.354	0.454	0.521
StdLSD_M (m/s)	0.810	0.935	0.818	1.124
MaxLSD_M (m/s)	4.050	5.323	3.850	5.953
AvgLSD_A (m/s)	1.112	1.116	1.324	1.703
StdLSD_A (m/s)	1.860	2.111	2.238	2.620
MaxLSD_A (m/s)	6.552	8.711	7.864	10.283

Tables 4 and 5 show the statistical indicators of longitudinal acceleration, i.e., “LA_M(A)”, and longitudinal jerk, i.e., “LJ_M(A)”, of vehicles M and A for the two control strategies in two scenarios, respectively. The results in Tables 4 and 5 show that the proposed CLC control strategy has significantly lower indicators as compared to the CACC_Sine control strategy except for the average longitudinal accelerations of vehicles M and A in two scenarios, and the average jerk of vehicle A in scenario 1. This further validates the conclusion obtained in Figures 9, 10, 14 and 15. The proposed CLC control strategy has more stable control inputs that greatly ensure the driving comfort.

Table 4. Indicator comparison for longitudinal accelerations of two control strategies.

Control Strategies Indicators	Scenario 1		Scenario 2	
	CLC	CACC_Sine	CLC	CACC_Sine
AvgLA_M (m/s ²)	0.166	0.166	0.067	0.066
StdLA_M (m/s ²)	0.459	0.805	0.674	1.144
MaxLA_M (m/s ²)	1.823	2.0	1.365	2.0
AvgLA_A (m/s ²)	0.067	0.066	0.033	0.033
StdLA_A (m/s ²)	0.974	1.521	1.071	1.516
MaxLA_A (m/s ²)	2.0	2.0	1.980	2.0

Table 5. Indicator comparison for longitudinal jerks of two control strategies.

Control Strategies Indicators	Scenario 1		Scenario 2	
	CLC	CACC_Sine	CLC	CACC_Sine
AvgLJ_M (m/s ³)	0.0052	0.0133	0.0133	0.0133
StdLJ_M (m/s ³)	0.0558	0.2304	0.0907	0.2573
MaxLJ_M (m/s ³)	0.3458	3.2520	0.5256	3.7890
AvgLJ_A (m/s ³)	−0.0067	−0.0067	0.0007	−0.0020
StdLJ_A (m/s ³)	0.1284	0.4651	0.1009	0.4087
MaxLJ_A (m/s ³)	0.3676	5.1104	0.4252	5.1577

4.3. Operating Efficiency Analysis of the Proposed CLC Control Strategy

A good CLC control strategy should not only have good control performance but also ensure considerable execution efficiency. The execution efficiency of a control strategy determines whether the control strategy is feasible to be embedded in an actual control module. It is usually evaluated by the control strategy computational simulation time and memory usage of the control strategy. These two indicators were also used in this study to evaluate the execution efficiency of the proposed CLC control strategy. In addition, since in this study, the proposed CLC control strategy is performed with 0.1 s as the execution cycle and the control inputs are obtained by continuously rolling-horizon optimization as time advances, the control strategy execution (computational) time and memory usage within each execution cycle are collected and analyzed of the above two lane change scenarios in this section.

The control strategy execution time and memory usage within each execution cycle for the entire simulation time in scenario 1 and scenario 2 are shown in Figures 16 and 17, respectively. From Figure 16, it can be found that the execution time of the proposed CLC control strategy in each execution cycle fluctuates mainly in the range of 0.06–0.075 s for both scenario 1 and scenario 2, and there are a few cases where the execution time is longer than 0.08 s. And the maximum execution time in both scenario 1 and scenario 2 is 0.089 s, and the average execution time are 0.064 s and 0.063 s, respectively, after statistical calculation. From the viewpoint of all execution durations in the whole simulation time, although there are fluctuations of a certain magnitude, the overall is less than 0.1 s, which can satisfy the minimum requirement of the algorithm embedded in the control module. In addition, the average execution times of 0.063 s and 0.064 s for the two scenarios are basically in line with the control application requirements, and the maximum execution time of 0.089 s is also an acceptable boundary value.

As shown in Figure 17, it can be easily found that the memory usage of the proposed CLC control strategy is mainly in the range of 0.08–0.20 MB in each execution cycle, with a few cases of more than 0.25 MB. This memory usage is overall in a reasonably acceptable range, and there are no drastic changes, indicating that the proposed CLC control strategy implementation has good stability. And the maximum memory usages in scenario 1 and scenario 2 are 0.367 MB and 0.340 MB, and the average memory usages are 0.1419 MB and 0.1388 MB, respectively. Due to the limitation of the hardware and computing capacity of the experimental computer equipment, there are cases that the memory consumption

is large in a few simulation cycles, but the overall memory consumption in the whole simulation cycle can be bounded within a reasonable range. Therefore, the proposed CLC control strategy can satisfy the basic requirements for implantation into embedded application devices.

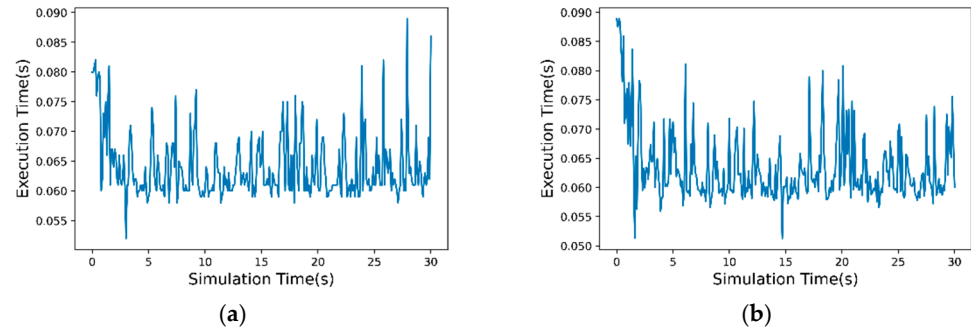


Figure 16. The execution time within each execution cycle of the proposed CLC control strategy for the entire simulation time in two lane change scenarios. (a) Scenario 1, (b) Scenario 2.

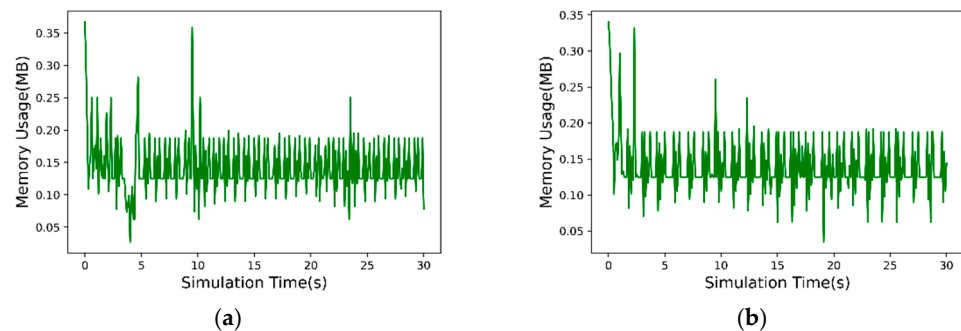


Figure 17. The memory usage within each execution cycle of the proposed CLC control strategy for the entire simulation time in two lane change scenarios. (a) Scenario 1, (b) Scenario 2.

In summary, both the execution time and memory usage of the proposed control strategy in each execution cycle are in a reasonable and acceptable range, which indicates the proposed CLC control strategy has good operating efficiency and can meet the basic requirements of the embedded system implantation algorithm.

5. Conclusions

This study proposes a CLC control strategy under a pure CAV traffic flow on a two-lane highway segment. It considers the correlation between the longitudinal and lateral motion of the lane change and the preceding vehicles switching problems of the controlled vehicles. The proposed CLC control strategy divides the lane-changing process into LC-O and LC-T stages based on the lateral position of the lane-changing vehicle. This effectively achieves the specific objective division of different stages of the lane change and reduces the complexity of the model solution. A preceding vehicle switching method using a set of linear piecewise functions based on a given lateral motion is designed to provide a smooth transfer when the preceding vehicles of the controlled vehicle changes. The proposed CLC control strategy is validated by comparing the CACC_Sine control strategy and with regard to the two typical lane change scenarios. The results show the proposed CLC control strategy has a good effect on vehicle switching tracking and can quickly realize the stable tracking of the target lane vehicles after changing lanes. Due to the real-time rolling optimization feature of MPC, the proposed CLC control strategy can also be applied to the scenario where the motion states of the preceding vehicles of two lanes change dynamically. Besides, the good operating efficiency makes the proposed CLC control strategy possible to be integrated into embedded control applications.

Firstly, the study scenario is based on pure CAV traffic flow and assumes that the motion states of leading vehicles on both lanes are known which is unrealistic the relevant research on the motion states of preceding vehicles will be explored in future work. Secondly, although the correlation between the movement of the two directions is considered in the model construction process, the lateral motion determined by the given trajectory function restricts the applicability of the model. In the future, we will consider constructing a preceding vehicle switching control strategy based on dynamic lane change lateral trajectories. Thirdly, the proposed CLC control strategy in this study is based on deterministic MPC, and uncertainties such as model prediction errors and control delays have not been considered. The introduction of these uncertainty factors in the model construction process will be considered in future work to make the model have better dynamic adaptability and robustness. Lastly, to further improve the efficiency of algorithm execution, we will do some memory optimization for the existing equipment and further optimize the algorithm code to keep the memory usage of the algorithm execution within the memory limit of the hardware equipment.

Author Contributions: Conceptualization, K.S., X.Z. and S.G.; methodology, K.S. and S.G.; validation, K.S. and X.W.; writing—original draft preparation, K.S.; writing—review and editing, K.S., S.G. and X.W.; funding acquisition, X.Z., S.G. and X.W. All authors have read and agreed to the published version of the manuscript.

Funding: This research is funded by National Key R&D Program of China (2019YFB1600100), NSFC (71901038), the 111 Project on Information of Vehicle-Infrastructure Sensing and ITS (B14043), Joint Laboratory for Internet of Vehicles (213024170015), Shaanxi Province Science Foundation (2020JQ-392, 2022JQ-663), China Postdoctoral Science Foundation (2022M710483), and Research funds for the Central Universities, Chang'an University (300102240301, 300102242103).

Institutional Review Board Statement: Not applicable.

Informed Consent Statement: Not applicable.

Data Availability Statement: Not applicable.

Acknowledgments: The authors are grateful to the reviewers' efforts and their valuable comments.

Conflicts of Interest: The authors declare no conflict of interest.

References

1. Zheng, Z.; Ahn, S.; Chen, D.; Laval, J. Freeway traffic oscillations: Microscopic analysis of formations and propagations using Wavelet Transform. *Transp. Res. Part B-Methodol.* **2011**, *45*, 1378–1388.
2. Ahn, S.; Cassidy, M.J. Freeway traffic oscillations and vehicle lane-change maneuvers. In Proceedings of the Transportation and Traffic Theory 2007, London, UK, 23–25 July 2007; pp. 691–710.
3. Barria, J.A.; Thajchayapong, S. Detection and classification of traffic anomalies using microscopic traffic variables. *IEEE Trans. Intell. Transp. Syst.* **2011**, *12*, 695–704.
4. Knipling, R.R. IVHS technologies applied to collision avoidance: Perspectives on six target crash types and countermeasures. In Proceedings of the 1993 Annual Meeting of IVHS America: Surface Transportation: Mobility, Technology, and Society, Washington, DC, USA, 14–17 April 1993; pp. 249–259.
5. Ammoun, S.; Nashashibi, F.; Laurgeau, C. An analysis of the lane changing manoeuvre on roads: The contribution of inter-vehicle cooperation via communication. In Proceedings of the 2007 IEEE Intelligent Vehicles Symposium, Istanbul, Turkey, 13–15 June 2007; pp. 1095–1100.
6. Talebpour, A.; Mahmassani, H.S. Influence of connected and autonomous vehicles on traffic flow stability and throughput. *Transp. Res. Part C-Emerg. Technol.* **2016**, *71*, 143–163.
7. Gong, S.; Zhou, A.; Peeta, S. Cooperative adaptive cruise control for a platoon of connected and autonomous vehicles considering dynamic information flow topology. *Transp. Res. Record.* **2019**, *2673*, 185–198. [\[CrossRef\]](#)
8. Ding, Y.; Zhuang, W.; Qian, Y.; Zhong, H. Trajectory planning for automated lane-change on a curved road for collision avoidance. In Proceedings of the WCX SAE World Congress Experience, Detroit, MI, USA, 9–11 April 2019. No. 2019-01-0673.
9. Zong, F.; He, Z.; Zeng, M.; Liu, Y. Dynamic lane changing trajectory planning for CAV: A multi-agent model with path preplanning. *Transp. B-Transp. Dyn.* **2022**, *10*, 266–292. [\[CrossRef\]](#)
10. Ghiasi, A.; Hussain, O.; Qian, Z.S.; Li, X. A mixed traffic capacity analysis and lane management model for connected automated vehicles: A Markov chain method. *Transp. Res. Part B-Methodol.* **2017**, *106*, 266–292. [\[CrossRef\]](#)

11. Dong, J.; Chen, S.; Li, Y.; Du, R.; Steinfeld, A.; Labi, S. Space-weighted information fusion using deep reinforcement learning: The context of tactical control of lane-changing autonomous vehicles and connectivity range assessment. *Transp. Res. Part C-Emerg. Technol.* **2021**, *128*, 103192.
12. Ma, C.; Hao, W.; Wang, A.; Zhao, H. Developing a coordinated signal control system for urban ring road under the vehicle-infrastructure connected environment. *IEEE Access* **2018**, *6*, 52471–52478.
13. Chen, Z.; Lin, X.; Yin, Y.; Li, M. Path controlling of automated vehicles for system optimum on transportation networks with heterogeneous traffic stream. *Transp. Res. Part C-Emerg. Technol.* **2020**, *110*, 312–329. [[CrossRef](#)]
14. Yao, H.; Li, X. Lane-change-aware connected automated vehicle trajectory optimization at a signalized intersection with multi-lane roads. *Transp. Res. Part C-Emerg. Technol.* **2021**, *129*, 103182.
15. Liu, J.; Zhao, W.; Xu, C. An efficient on-ramp merging strategy for connected and automated vehicles in multi-lane traffic. *IEEE Trans. Intell. Transp. Syst.* **2021**, *23*, 5056–5067.
16. He, Y.; Sun, D.; Zhao, M.; Cheng, S. Cooperative driving and lane changing modeling for connected vehicles in the vicinity of traffic signals: A cyber-physical perspective. *IEEE Access* **2018**, *6*, 13891–13897. [[CrossRef](#)]
17. Heesen, M.; Baumann, M.; Kelsch, J.; Nause, D.; Friedrich, M. Investigation of cooperative driving behaviour during lane change in a multi-driver simulation environment. In Proceedings of the Human Factors and Ergonomics Society (HFES) Europe Chapter Conference Toulouse, Boston, MA, USA, 22–26 October 2012; pp. 305–318.
18. Lin, D.; Li, L.; Jabari, S.E. Pay to change lanes: A cooperative lane-changing strategy for connected/automated driving. *Transp. Res. Part C-Emerg. Technol.* **2019**, *105*, 550–564.
19. Cao, W.; Mukai, M.; Kawabe, T.; Nishira, H.; Fujiki, N. Cooperative vehicle path generation during merging using model predictive control with real-time optimization. *Control Eng. Pract.* **2015**, *34*, 98–105. [[CrossRef](#)]
20. Nie, J.; Zhang, J.; Ding, W.; Wan, X.; Chen, X.; Ran, B. Decentralized cooperative lane-changing decision-making for connected autonomous vehicles. *IEEE Access* **2016**, *4*, 9413–9420.
21. Wang, G.; Hu, J.; Li, Z.; Li, L. Cooperative lane changing via deep reinforcement learning. *arXiv* **2019**, arXiv:1906.08662.
22. Xu, M.; Luo, Y.; Yang, G.; Kong, W.; Li, K. Dynamic cooperative automated lane-change maneuver based on minimum safety spacing model. In Proceedings of the 2019 IEEE Intelligent Transportation Systems Conference (ITSC), Auckland, New Zealand, 27–30 October 2019; pp. 1537–1544.
23. Goli, M.; Eskandarian, A. MPC-based lateral controller with look-ahead design for autonomous multi-vehicle merging into platoon. In Proceedings of the 2019 American Control Conference (ACC), Philadelphia, PA, USA, 10–12 July 2019; pp. 5284–5291.
24. Guo, N.; Zhang, X.; Zou, Y.; Lenzo, B.; Zhang, T. A computationally efficient path-following control strategy of autonomous electric vehicles with yaw motion stabilization. *IEEE Trans. Transp. Electrification* **2020**, *6*, 728–739. [[CrossRef](#)]
25. Dini, P.; Saponara, S. Processor-in-the-loop validation of a gradient descent-based model predictive control for assisted driving and obstacles avoidance applications. *IEEE Access* **2022**, *10*, 67958–67975. [[CrossRef](#)]
26. Cosimi, F.; Dini, P.; Giannetti, S.; Petrelli, M.; Saponara, S. Analysis and design of a non-linear MPC algorithm for vehicle trajectory tracking and obstacle avoidance. In Proceedings of the Applications in Electronics Pervading Industry, Environment and Society: APPEPIES 2020, Online, 19–20 November 2020; Springer International Publishing: Berlin, Germany, 2021; pp. 229–234.
27. Wang, D.; Hu, M.; Wang, Y.; Wang, J.; Qin, H.; Bian, Y. Model predictive control-based cooperative lane change strategy for improving traffic flow. *Adv. Mech. Eng.* **2016**, *8*, 1687814016632992.
28. Li, B.; Zhang, Y.; Feng, Y.; Zhang, Y.; Ge, Y.; Shao, Z. Balancing computation speed and quality: A decentralized motion planning method for cooperative lane changes of connected and automated vehicles. *IEEE T. Intell. Veh.* **2018**, *3*, 340–350. [[CrossRef](#)]
29. Li, T.; Wu, J.; Chan, C.; Liu, M.; Zhu, C.; Lu, W.; Hu, K. A cooperative lane change model for connected and automated vehicles. *IEEE Access* **2020**, *8*, 54940–54951.
30. Ni, J.; Han, J.; Dong, F. Multivehicle cooperative lane change control strategy for intelligent connected vehicle. *J. Adv. Transp.* **2020**. [[CrossRef](#)]
31. Luo, Y.; Yang, G.; Xu, M.; Qin, Z.; Li, K. Cooperative lane-change maneuver for multiple automated vehicles on a highway. *Automot. Innov.* **2019**, *2*, 157–168.
32. Du, R.; Chen, S.; Li, Y.; Dong, J.; Ha, P.Y.J.; Labi, S. A cooperative control framework for CAV lane change in a mixed traffic environment. *arXiv* **2020**, arXiv:2010.05439.
33. Nie, G.; Xie, B.; Lu, H.; Tian, Y. A cooperative lane change approach for heterogeneous platoons under different communication topologies. *IET Intell. Transp. Syst.* **2022**, *16*, 53–70.
34. Wang, Z.; Shi, X.; Zhao, X.; Li, X. Modeling decentralized mandatory lane change for connected and autonomous vehicles: An analytical method. *Transp. Res. Part C-Emerg. Technol.* **2021**, *133*, 103441. [[CrossRef](#)]
35. Zheng, Y.; Ran, B.; Qu, X.; Zhang, J.; Lin, Y. Cooperative lane changing strategies to improve traffic operation and safety nearby freeway off-ramps in a connected and automated vehicles environment. *IEEE Trans. Intell. Transp. Syst.* **2019**, *21*, 4605–4614.
36. Luo, Q.; Nguyen, A.T.; Fleming, J.; Zhang, H. Unknown input observer based approach for distributed tube-based model predictive control of heterogeneous vehicle platoons. *IEEE Trans. Veh. Technol.* **2021**, *70*, 2930–2944. [[CrossRef](#)]
37. Bai, Y.; Zhang, Y.; Hu, J. A motion planner enabling cooperative lane changing: Reducing congestion under partially connected and automated environment. *J. Intell. Transport. Syst.* **2021**, *25*, 469–481. [[CrossRef](#)]

38. Tian, D.; Luo, H.; Zhou, J.; Wang, Y.; Yu, G. A self-adaptive V2V communication system with DSRC. In Proceedings of the 2013 IEEE International Conference on Green Computing and Communications and IEEE Internet of Things and IEEE Cyber, Physical and Social Computing, Beijing, China, 20–23 August 2013; pp. 1528–1532.
39. Sun, K.; Zhao, X.; Wu, X. A cooperative lane change model for connected and autonomous vehicles on two lanes highway by considering the traffic efficiency on both lanes. *Transp. Res. Interdiscip. Perspect.* **2021**, *9*, 100310. [[CrossRef](#)]
40. Chovan, J.; Tijerina, L.; Alexander, G.; Hendricks, D.L. *Examination of Lane Change Crashes and Potential IVHS Countermeasures*; Final Report 1994; No. HS-808 071; ROSAP: Copenhagen, Denmark, 1994.
41. Katrakazas, C.; Quddus, M.; Chen, W.H.; Deka, L. Real-time motion planning methods for autonomous on-road driving: State-of-the-art and future research directions. *Transp. Res. Part C-Emerg. Technol.* **2015**, *60*, 416–442.
42. Coppola, A.; Lui, D.G.; Petrillo, A.; Santini, S. Cooperative Driving of Heterogeneous Uncertain Nonlinear Connected and Autonomous Vehicles via Distributed Switching Robust PID-like Control. *Inf. Sci.* **2023**, *625*, 277–298. [[CrossRef](#)]
43. Hult, R.; Sadeghitabar, R. Path Planning for Highly Automated Vehicles. Master's Thesis, Chalmers University of Technology, Gothenburg, Sweden, 2013.
44. Hart, W.E.; Laird, C.D.; Watson, J.P.; Woodruff, D.L.; Hackebeil, G.A.; Nicholson, B.L.; Siirola, J.D. *Pyomo-Optimization Modeling in Python*; Springer: Berlin, Germany, 2017; Volume 67, p. 277.
45. VanderWerf, J.; Shladover, S.; Kourjanskaia, N.; Miller, M.; Krishnan, H. Modeling effects of driver control assistance systems on traffic. *Transp. Res. Record.* **2001**, *1748*, 167–174. [[CrossRef](#)]
46. Mar, J.; Lin, H.T. The car-following and lane-changing collision prevention system based on the cascaded fuzzy inference system. *IEEE Trans. Veh. Technol.* **2005**, *54*, 910–924.

Disclaimer/Publisher's Note: The statements, opinions and data contained in all publications are solely those of the individual author(s) and contributor(s) and not of MDPI and/or the editor(s). MDPI and/or the editor(s) disclaim responsibility for any injury to people or property resulting from any ideas, methods, instructions or products referred to in the content.